Master Thesis, Department of Geosciences

Micro CT scanning of a new specimen of the Zygodactylidae (Aves) from the Early Eocene of Messel, Germany

Christian Haugen Svendsen

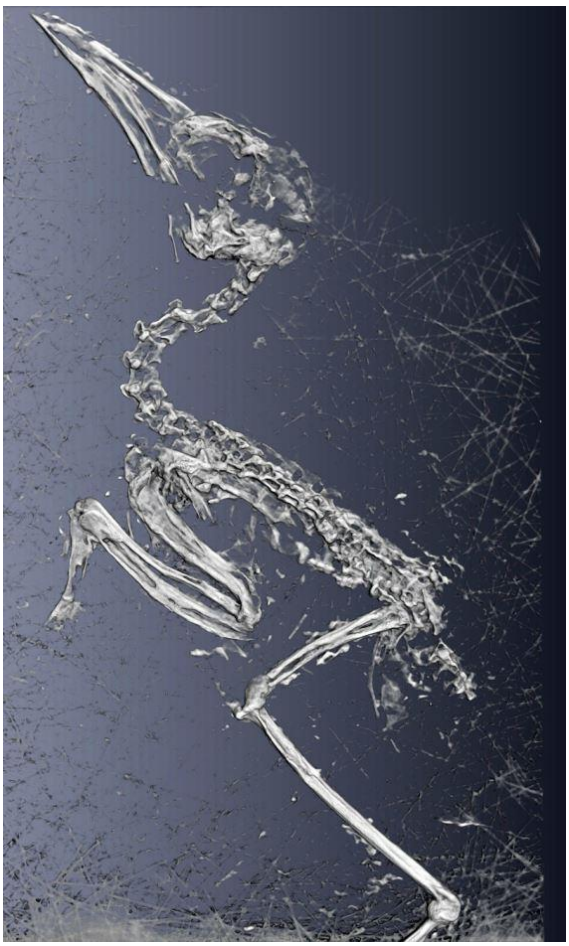

UNIVERSITY OF OSLO

FACULTY OF MATHEMATICS AND NATURAL SCIENCES

Micro CT scanning of a new specimen of the Zygodactylidae (Aves) from the early Eocene of Messel, Germany

Christian Haugen Svendsen

Master Thesis in Geosciences

Discipline: Palaeontology

Department of Geosciences and Natural History museum, Oslo

Faculty of Mathematics and Natural Sciences

University of Oslo

September 2015

Acknowledgement

I want to thank and dedicate this work to my aunt *Rita*. Thanks for taking me to the Natural History Museum in Oslo when I was just a small kid. You helped me to get a general interest in the Evolution of life, and how complex we are, and this gave a 7 year old boy a dream. A dream to become a Palaeontologist!

First and foremost I would like to thank my two excellent supervisors, *Jørn Hurum* and *Gerald Mayr*. Thanks for helping me whenever I had questions and for your suggestions on the thesis. Your patience, readiness and excellent guidance were crucial for this thesis. Special thanks to *Gerald* for meeting me in Frankfurt on my trip there, and showing me the collection at the Senckenberg museum.

I want to thank the Senckenberg museum in Frankfurt for letting me examine the bird fossils from their records for my thesis.

I greatly appreciate the help from Øyvind Hammer for the help with the CT scanning, and teaching me the basics of Avizo software. Thanks also to Aubrey Roberts, who introduced me to 3D modelling, and helped me whenever I had problems with the software.
I also want to thank my old English teacher Bjarne, for proof-reading the final draft.

Many thanks to all my friends for all gatherings, parties and coffee breaks. Thanks to my family that always supports me. Special thanks to my girlfriend *Elisabeth*, for listening and always being critical to my thesis. Thanks for proof-reading early drafts of the text.

Abstract

Representatives of the avian taxon Zygodactylidae are among the best known small arboreal birds from the early Palaeogene. Still, however, the anatomy of zygodactylids is not fully understood. It is therefore important that new anatomical elements are observed and studied in detail to further support their position within the modern phylogenetic system of birds. In this study an almost complete specimen of the Zygodactylidae from the Early Eocene of Messel, Germany has been studied. This fossil belongs to the species *Primozygodactylus major*, and for the first time a Messel bird was investigated with a micro computed tomography (CT) scanner. This is the third known specimen of *P. major* and is compared with previously described zygodactylids from various fossil localities (Messel, Germany, Green River Formation, Wyoming, USA and Luberon area, Southern France) and extant "higher land birds". This study is the first to create a three-dimensional model of the quadrate and the os carpi radiale of the Zygodactylidae. The quadrate shows a resemblance to previously examined specimens of the Zygodactylidae, but also shows unique characters only seen in the Upupiformes (wood hoopes and hoopes). The following are new anatomical characters of *Primozygodactylus major* observed in PMO 212.659; Quadratum: The capitulum squamosum is situated higher than the capitulum oticum, with a small slope between them, and no vallecular intercondylaris is present, the capitulum oticum has an extensive medial protrusion, the laterocaudal condyle ends with a sharp-edged flange, a shallow depression on the cotyla quadratojugalis, the medial condyle exceeds the lateral condyle ventrally, a large laterocaudale condyle, with a small depression between the lateralocaudal and medial condyle, and is most likely a lateral trochlea on the medial condyle. Os carpi radiale: shows similarities to the other Zygodactylidae, *Zygodactylus luberonensis*, and to some of the Coraciiformes.

Contents

1. Introduction

1.1 Messel

The Messel pit is situated on the Sprendlinger Horst, the northern extension of the Odenwald basement, which lies in contact with the Upper Rhine Graben, approximately 9 kilometers northeast of Darmstadt in Germany (Schaal & Ziegler, 1992). This site was once a quarry where bituminous shale was mined. Brown coal and later oil shale was actively mined from the 1850s and onwards. It was not until the early 1900s the pit became known for the abundance of excellent preservation of fossils, where an entire ecosystem was captured (Schaal & Ziegler, 1992).

The first systematic scientific excavations started in the 1970s. When the oil shale mining ceased in 1971, the unoccupied land was slotted for use as landfill, but the plans came to a halt because of local demonstration and hard criticism from the scientific community. As a result, the Hessian state bought the site in 1991 to secure the scientific access (Schaal & Ziegler, 1992). Due to the extraordinary fossils, the pit was declared a UNESCO world heritage site in 1995 (Schaal & Schneider, 1995).

1.1.1 Messel fossils

Messel is known for having extraordinary preserved fossils, but what makes it spectacular is the abundance of a multitude of different species (Franzen, 1985). With a great diversity of organisms, from plants to fish, amphibians, reptiles, birds and mammals, the Messel pit has captured an entire ecosystem (Schaal & Ziegler, 1992). The reason why there is such an abundance of animals fossilized in the Messel pit can be explained by the periodic events of gas outlet from the maar volcano, which poisoned the animals living in or by the lake. The bottom of the lake was probably anoxic, and is why the fossils are well-preserved (Franzen, 1985). The anoxic bottom halted the decay of the organisms, so no abrupt burial was needed. All of the Messel fossils are slightly crushed, due to the deformation of the surrounding oil shale. The oil shale found in Messel is largely composed of smectites, and smectites are easily deformed (Buness et al., 2005), thus the clays internal structure collapses under

pressure. When the oil shale is obtained it contains a high percentage of water, and if it is allowed to dry, it will crumble, making the Messel fossils in need of a special preservation method (Micklich & Drobek, 2007). The method used is based on transferring the fossil to a new matrix. This transfer method was first developed by Kühne (1961), and in the early stages of this method it was common to use polyester resin to make the artificial matrix, but it was later replaced due to the shrinking problems, and today it is made up by epoxy resin (Micklich & Drobek, 2007; Selden & Nudds, 2012).

1.1.2 Messel birds

Avian fossils are generally rare, but the Messel fossil site has produced a large quantity of bird fossils (Franzen, 1985). Many of the ecological niches were left empty after the extinction of the dinosaurs and pterosaurs at the end of the Cretaceous. These were filled by mammals and birds during the Cenozoic. By the middle of the Eocene Epoch, nearly all of the orders of mammals and major groups of birds had evolved (Feduccia, 2003). The Messel pit reflects this, with bird fossils from Messel showing an enormous diversity in both genera and species, belonging to more than 30 families. These bird fossils are similar to the orders, Struthioniformes, Galliformes, Gruiformes, Podargiformes, Nyctibiiformes, Apodiformes, and Upupiformes (Reimann, 2007; Schaal, 2012). Many of the bird groups that are found in Messel are now extinct, but are closely related to modern orders. The avian fauna from Messel represents the terrestrial and arboreal birds that lived close to Lake Messel. Shorebirds, however, are rare and only known from a fragmentary specimen. The single bird species known from Messel that is adapted to a life in water is *Juncitarsus*, a tall, long-legged bird, which is closely related to Phenicoteriformes (Mayr, 2005b). The variety of bird species in the Messel fauna reflects the habitat, with Lake Messel having been situated in a paratropical forest. The fossils include feather remains, stomach content as well as complete articulated skeletons (Franzen, 1985). All Messel fossils are more or less flattened, but sometimes some of the bones survive the flattening and crushing processes, and three dimensional bones are preserved (Micklich & Drobek, 2007).

Like today, small birds make up the most of the avian species, and most of the birds that are found in Messel are small to very small in size, ranging from 7.5 cm to 30.0 cm.

1.2 Higher land birds

Molecular analysis the last decade indicates a Cretaceous origin of many neornithines, and DNA sequence data have clarified many interfamily relationships of higher level groups, and have supported various clades, such as aquatic, higher landbird assemblage, shorebirds and passerines (Ericson et al., 2006).

The largest clade in neornithines is the Passeriformes, which represents more than half of all avian species. Passeriformes can be divided into three suborders; Oscines, Suboscines and Acanthisittidae, and these birds are typically small to medium sized birds. Passeriformes have an abundant Neogene fossil record, but a sparse one in the Paleogene (Mayr, 2005a, 2009). All Paleogene remains are from the Oligocene of Europe (Bochenski et al., 2011; Mayr & Manegold, 2004) . Molecular analysis suggest a sister group relationship between Passeriformes and the Psittaciformes (Ericson et al., 2006; Hackett et al., 2008; Jarvis et al., 2014). This is interesting, since the Passeriformes were shown to be the sister taxon of the Zygodactylidae. Zygodactylids are zygodactyl, which is similar to that of the Psittaciformes, and this opens for the possibility that a zygodactyl foot is plesiomorphic for the clade Psittacopasserae, including Passeriformes and Psittaciformes and was secondarily lost in Passeriformes (Botelho et al., 2014) (see Figure 1). A zygodactyl foot is a common trait of many arboreal birds today and most likely developed independently in many bird taxa (Olson, 1983) (see Figure 1).

It is a discussion on what the sister taxon of the Passeriformes is, and previous authors considered them closest to either the Piciformes or Coraciiformes (Cracraft, 1988; Fain, Houde, & Harrison, 2004; Livezey & Zusi, 2007). However, the Piciformes show a strong relationship with the Coraciiformes, and the Piciformes were placed by Hackett et al. (2008) as a subgroup within the Coraciiformes. Mayr (2011) later termed this clade Picocoraciae. The Picocoraciae includes the Coraciiformes *sensu stricto*, Alcediniformes, Piciformes and Bucerotes. The Piciformes are known best for being perching birds with zygodactyl foot, and are separated into two suborders Galbulae and Pici (see Figure 1). The earliest recorded modern-type piciform stems from the late Oligocene (Mayr, 2001), which is similar to observations in the Passeriformes.

The fossil record suggests an early Paleogene diversification of neornithines, but the early evolution of Neornithes is not fully understood, and a study of extinct bird taxa is of crucial importance (Chiappe & Witmer, 2002).

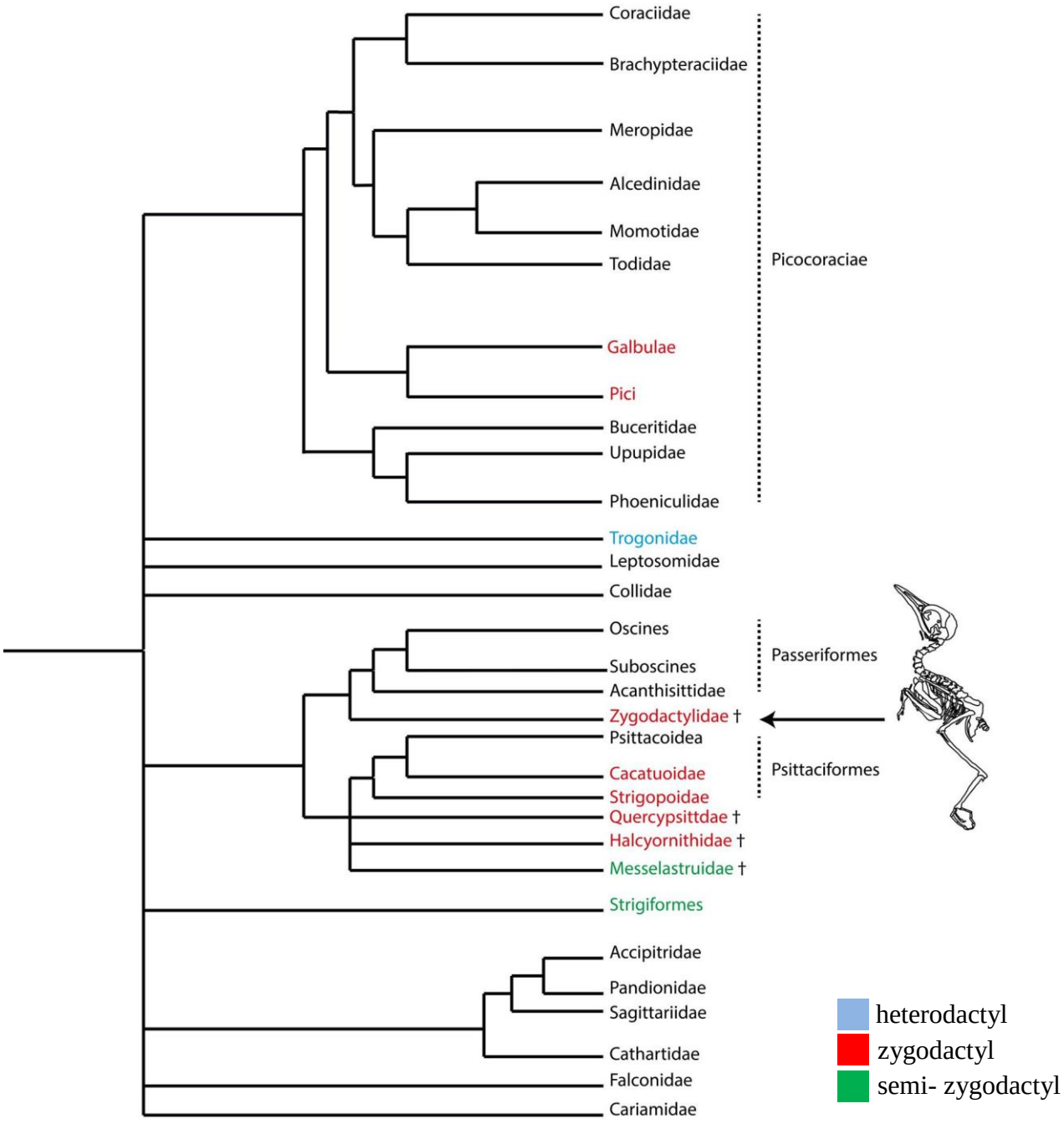

Figure 1: ***Phylogenetic studies have led to the conclusion that the Zygodactylidae is the sister taxon of the Passeriformes. This particular phylogenetic tree also shows the "landbird assemblage", and the distribution of zygodactyl feet in the different taxa. The illustration shows the position of PMO 212.659 within the cladogram; figure modified from Botelho et al., (2014) and (Mayr, 2011).***

1.3 Zygodactylidae

Zygodactylidae is an extinct avian taxon, with a stratigraphic occurrence from Eocene to Miocene, which is about 30 million years. There are currently four main genera placed within the Zygodactylidae: *Zygodactylus, Primoscens*, *Primozygodactylus* and *Eozygodactylus.* The first taxon to be described was *Zygodactylus*, which was described by Ballmann (1969a, 1969b) based on specimens from the Early Miocene of Germany and Middle Miocene of France. At that time *Zygodactylus* was only known from distal tibiotarsi and tarsometatarsi (Ballmann, 1969a, 1969b). Ballmann considered the systematic position of *Zygodactylus* uncertain. Because of the uncertain phylogenetic affinities of *Zygodactylus*, Brodkorb (1971) created a new family, the Zygodactylidae and placed it within the Piciformes. All zygodactylids share a large trochlea accessoria (Mayr, 1998, 2008; Weidig, 2010), which can be seen in extant Psittaciformes and Piciformes and suggest that the fourth toe was zygodactyl (Mayr, 2003). A similar taxon of a small bird from the early Eocene was described by Harrison and Walker (1977), and created the family "Primoscenidae". At that time it contained only one species, *Primoscens minitus* from the Early Eocene London Clay, England (Harrison & Walker, 1977). This species was only known from an incomplete carpometacarpus, but later more skeletal elements were identified by Mayr (1998). Mayr (1998) described a new genus of "Primoscenidae" *Primozygodactylus* from the Early Eocene of the Messel fossil site. *Primozygodactylus* are one of the most abundant small fossil birds from the Messel fossil site (Mayr & Zelenkov, 2009). There are currently four recognized species of *Primozygodactylus* from the Messel site: *Primozygodactylus danielsi, P. ballmanni, P. eunjooae* and *P. major* (Mayr, 1998; Mayr & Zelenkov, 2009). Where *P. danielsi* is the smallest and *P. major* is the largest of them. Almost all *Primozygodactylus* are found as articulated skeletons with three-dimensional bones preserved (Mayr, 1998).

Mayr, recognized the similarities between the Primoscenidae and the Zygodactylidae, and suggested a possible sister taxon relationship of the Primoscenidae with the clade Zygodactylidae and Piciformes (Mayr, 1998, 2004).

Subsequently, Mayr (2004) performed a more detailed analysis of the affinities of "primoscenids" and recovered a sister group relationship between the Passeriformes and the clade Zygodactylidae + Primoscenidae (Mayr, 2004). In 2008, the first nearly complete skeleton of *Zygodactylus* was described from the Early Oligocene in Luberon, France and this further supported the presumed sister group relationship with the Passeriformes. Based on these studies, "Primoscenidae" was recognized as a junior synonym of the Zygodactylidae (Mayr, 2008).

The first Zygodactylidae from North America was described by Weidig (2010). The genus *Eozygodactylus* was found in Green River Formation, Wyoming, USA.

The morphology of the hypotarsus of the Zygodactylidae differs from that of the Piciformes and is more like that of the the Passeriformes. In particular, the hypotarsal canal for the musculus flexor hallucis longus in the hypotarsus is closed in the zygodactylids (Mayr, 2004, 2008), in contrast to an open canal in the Piciformes. The open canal is believed to further support the retroverted toe (Swierczewski & Raikow, 1981). The zygodactyl foot bears a large trochlea accessoria, and is used for classification within the Zygodactylidae. In zygodactylids, the size and shape of the trochlea accessoria varies. It is small in *Primozygodactylus*, but very large and distally elongated in *Zygodactylus*. The trochlea accessoria of *Zygodactylus* is similar to the Piciformes, but is larger in size (see description).

A key feature of the Zygodactylidae is found on the carpometacarpus. This bone is one of the most characteristic bones of the Zygodactylidae. It is short, stout and possesses a well-developed processus intermetacarpalis, which is fused to the os metacarpale minus (Mayr, 1998). A processus intermetacarpalis is one of the synapomorphies of Zygodactylidae and Passeriformes (Mayr, 1998, 2008). Apparently this feature evolved convergently in Piciformes, which also possess an intermetcarpal process (Mayr & Manegold, 2004). Still, however, the anatomy of zygodactylids is not fully understood, because many osteological details are not clearly visible in the known specimens.

1.4 Micro Computed Tomography

Only a few months after W. C. Röntgen discovered "the x-rays", the first x-rays of fossils were performed in Berlin (Brühl, 1896) and in Paris (Lemoine, 1896). At that time this was rather sporadic, and it was not until the 1960s that x-ray studies became common in palaeontology (Habersetzer, 1995). Messel fossils were first x-rayed in the 1980s, and since then Senckenberg Research Institute has been a frontier for x-ray studies on fossils (Habersetzer, 1995).

X-ray is a well-known method of acquiring data of bones that are hidden by sediment or other bones. The method has been improved over decades, but even with improvement it has its limitations. It projects the image in a 2D format, making some details hard to see if the contrasts are the same (e.g. bone overlying bone). The new innovative method for x-ray is computed tomography (CT) scanning, which is mostly used for medical purposes, but has proved to be a valuable application for paleontological research. The uses of micro CT scans have become increasingly more popular in palaeontology. A micro CT scan operates on the same principles as the conventional CT scanner, only it is smaller and cannot take large objects, but has stronger current. The main advantage with a micro CT scanner is the ability to get three-dimensional images in a non-destructive way (Cnudde & Boone, 2013), allowing detailed studies of specimens in a fixed position in the matrix (Franzen *et al.*, 2009). This is the reason why micro CT scan is so important for Messel fossils, since the bones in Messel specimens often are lightly crushed. The crushed bones limit the possibilities for freely preparing the bones and must therefore be studied in a fixed position.

A micro CT scanner gets its data by having x-ray tubes fixed, while the object of interest is slowly rotating. The emitting x-rays from the tubes traverses through a cross section of the object to generate attenuation profiles at the detector (Kalra et al., 2004). The X-ray beam projects around the area of interest, and a software that can assemble the cross-sectional images into three-dimensional projections by calculating data points in relation to the surrounding points for each location (Rogers, 1999). The image quality is controlled by the current in the x-ray tube. Higher current equals better image quality, but higher radiation. This is a problem when using it on live specimens, but unlike the conventional CT scan (which is used on live specimen), the micro CT scanner is used on skeletons, drill cores and

fossils (Cnudde & Boone, 2013; Mees et al., 2003) and thus, the image quality versus radiation exposure is not an issue. Even though the CT scanner is a powerful tool, it also has its limitations. Like all imaging techniques, x-ray images are subjects to noise (Cnudde & Boone, 2013). The drawback with a high resolution scan is that the sample has to be small, and many individual scans must be done. Another limitation using micro CT scan is that it is costly, and that the interpretation and the process of obtaining useful data are time-consuming.

1.4.1 Micro computed tomography of other fossil specimens

The micro CT scan has been applied on various specimens from the Messel fauna, with the most famous of these being the primate *Darwinius masillae* (Franzen et al., 2009). In this specimen, the CT-scan helped to locate teeth that were not visible for the naked eye, and helped to age assess the specimen. Most fossils from Messel that were previously analyzed with this method were, however, mammals, and for birds no CT studies exist. In the present study, a fossil bird from Messel is for the first time analyzed with a CT scanner.

1.5 Site description

The oil shale of Messel is among the best known isolated Palaeogene deposit (Felder et al., 2001) . The Messel pit is located on an uplifted block of igneous and metamorphic rocks of Carboniferous age, which is covered by lower Permian sediments. The lake sediments of the Messel pit were defined as the "Messel formation", which mainly consists of highly bituminous shale (Lenz et al., 2008, 2011). The Messel deposited are in a maar-crater, which is approximately 1000 m long, 700 m wide and 200 m deep (Schaal & Ziegler, 1992). It was proven to be a maar crater when a hole was drilled 433 meter in the center of the pit in 2001 ("Messel 2001") (Gabriele, 2007). The layering of the drill core was as follows; lacustrine oil shale with a thickness of 140 m overlying 90 m of clastic lake sediments. These units are divided into middle and lower Messel formation, respectively (Lenz et al., 2007). The lacustrine deposits are followed by volcanoclastic rocks, such as lapilli tuffs, continuing to a depth of 373 m, and volcanic breecias to a depth of 433 m (Gabriele, 2007). A maar volcano is created when groundwater and hot magma come into contact with each other (Selden &

Nudds, 2012). Eruptions from a maar volcano consist mainly of gas, water and volcanic debris. Maar volcanoes produce craters in which groundwater and rainwater slowly accumulate, and become freshwater lakes (Schaal, 2012). The base of the Messel formation consists of gravel and sand, which represents the early formation of the basin where there was high energy fill resulting from screes at the edge of the basin, and/or river activity. The oil shale overlies the sand and gravel, representing quieter conditions of sedimentation, and probably stems from the time when the lake had formed. Occasional layers of coarser material, as sand or gravel, can be seen within the oil shale sequence. These layers are created by occasional screes from the edge of the basin (Gabriele, 2007).

Several time series analyses have been done on the oil shale and have led to the assumption of an annual varve-like stratification (Lenz et al., 2011). This was originally suggested by Irion (1977) and further supported by Goth (1990) who studied the distribution of palynomorphs in individual laminae, and determined the sedimentation rate to be 0.15mm/year by counting oil laminae. El bay et al. (2001) calculated similar data from an older well, with an sedimentation rate of 0.146 ± 0.052 mm/year, and the new core from "Messel 2001" indicated a sedimentation rate of 0.14 mm/year (Schulz et al. 2002). From that sedimentation rate it has been calculated that it took 1.1 million years to deposit the 140 m of biotuminous shale that was recorded in the core Messel 2001 (Lenz et al., 2007; Shulz et al., 2002).

The lower and upper unit in the Messel formation is of coarser material and worked as a shield and helped to preserve the fossils in the middle unit, the highly laminated oil shale (Schaal & Ziegler, 1992). The present day oil shale consists of clay minerals (35 %), organic matter (25 %), and water (40 %) (Buness et al., 2005). The most important mineral of the oil shale are smectites, which is a group of highly absorbent clay minerals capable of absorbing large amount of water (Buness et al., 2005), and this is why the oil shale is "wet" when it is mined. The Messel formation can only be traced a few kilometers from the Messel pit, because it is restricted by lake basins within the Rhine rift valley (Gabriele, 2007; Schaal & Ziegler, 1992; Selden & Nudds, 2012). The Messel fauna was previously dated to be from the middle Eocene (Geiseltalian), MP11 (Franzen, 2005), radiometric age has been calculated to be approximately 47.8 Ma, based on basalt fragments from the underlying volcanic chimney (Mertz & Renne, 2005). However, a recent study has revealed that the

volcanic eruption at Messel happened between 48.27 ± 0.22 and 48.11 ± 0.22 Ma (Lenz et al., 2015). This means that the Messel oil shale is slightly older than previously assumed and that the European Land Mammal Age Geiseltalian (MP 11) boundary moves into the lower Eocene.

Messel was situated further south in the Eocene, close to where Spain is located today (Schaal, 2012). During the Palaeocene the temperature rose and is the most recent "greenhouse" climate that climaxed in the Early Eocene. After the Early Eocene Climate Optimum, a general cooling followed, however, there were periods of hyperthermal events, and the most prominent is the Palaeocene/Eocene Thermal Maximum (PETM), an episode of ~ 200 kyr of extreme global warming (Kenneth & Slott, 1991; Baines et al., 2000; Röhl et al., 2000). This is reflected in the Messel pit sedimentation, and the rich flora and fauna captured as fossils (Lenz et al., 2011) .

1.6 Aim

Numerous remains of the Zygodactylidae have been discovered and described, both in Europe and in North America, but many questions still remain. Most of the articulated skeletal remains are found in the Messel pit with many complete skeletons (Mayr, 1998; Mayr & Zelenkov, 2009) and more recently in the Green River Formation (Weidig, 2010). There is little known about the osteology of the cranium (internal and external), and some features of the pectoral and pelvic region remains uncertain.

There have been several phylogenetic studies of birds (Cracraft, 1988; Ericson et al., 2006; Fain et al., 2004; Hackett et al., 2008; Jarvis et al., 2014; Livezey & Zusi, 2007; Mayr, 2004, 2008). Neornithines are already highly evolved in the early Palaeogene, and reflects an early diversification early in their evolutionary history (Hackett et al., 2008). Palaeobiological and molecular evidence support such a rapid radiation for neornithines (Jarvis et al., 2014). The problem with such a rapid radiation is that it makes it difficult to recover deep evolutionary relationships. This diversification has resulted in many distinctive, morphologically cohesive groups with few extant intermediary forms linking them to other well-defined groups (Hackett et al., 2008). This is why it is important to study fossil birds.

Fossil birds, like the Zygodactylidae, can help us understand the early radiation of birds and their complex interrelationship.

In this thesis, a description of a nearly complete articulated specimen of *Primozygodactylus major* will be given. *P. major* is only known from two previously described specimens. The first is an almost complete skeleton (SMF-ME 1758a+b) (Mayr, 1998), while the second is only partly preserved (SMF-ME 799a+b) and one of the few *Primozygodactylus* that are dissociated (Mayr & Zelenkov, 2009). The aim is to obtain new morphological data and to give further insight to already known features. The second aim of the thesis is to test the application of a micro CT scanner on the specimen and if it can reveal further morphological data that cannot be studied with stereo microscopes. It worth noting that this is the first time a bird from the Messel pit has been scanned by a micro CT scanner.

2. Material & Methods

The specimen PMO 212.659 (Plate A) is from Messel near Darmstadt, Germany, from the type horizon MP 11, Grube Messel, Early Eocene. The counterpart is in the private Perner collection and will be referred to as Plate B. Plate B has only been studied based on a high resolution image (see Figure 2), so it was not possible to discern all details.

Figure 2: ***Specimens of* Primozygodactylus major *Mayr, 1998 from early Eocene of Messel in Germany. Left is PMO 212.659 (Plate A), right is the counter slab of the same fossil from the private Perner collection (Plate B). Only the left specimen was available for this study.***

Osteological terminology follows Baumel and Witmer (1993), except for the quadrate and the os carpi radiale. The terminology of the os carpi radiale follows Mayr (2014) and that of the quadrate follows Elzanowski and Boles (2015). The measurements are in

millimeters, and represent the maximum length of the bones along their longitudinal axes. Measurements were taken with a digital caliper.

Comparative material that was used in this study was observed and studied at the Senckenberg Museum, Germany. Specimens that were studied: *Primozygodactylus major* (SMF-ME 1758a [holotype]), *Primozygodactylus danielsi* (SMF-ME 2522a+b [holotype], SMF-ME 2383a+b), *Primozygodactylus eunjooae* (SMF-ME 1074 [holotype]) and *Primozygodactylus ballmanni* (SMF-ME 2108 [holotype]). In addition to the *P. major* holotype, specimen SMF-ME 799a+b was also used for comparison, but it was not directly examined by me, with the measurements and details taken from Mayr and Zelenkov, (2009).

2.1 Micro Computed Tomography Scanner

A micro Computed Tomographic (CT) scanner was used to get an accurate osteological reconstruction of the specimen PMO 212. 659 (see Figure 3). The fossil was scanned with a Nikon Metrology XT H 225 ST microfocus CT scanner at the Natural History Museum in Oslo, with the X-ray source running at 140 kV and 200 mA, and with a 0.25 mm tin X-ray filter. The software used for the reconstructions and volume analysis is the Avizo Fire 8.1. Avizo is a three dimensional data processing, modeling and analysis software.

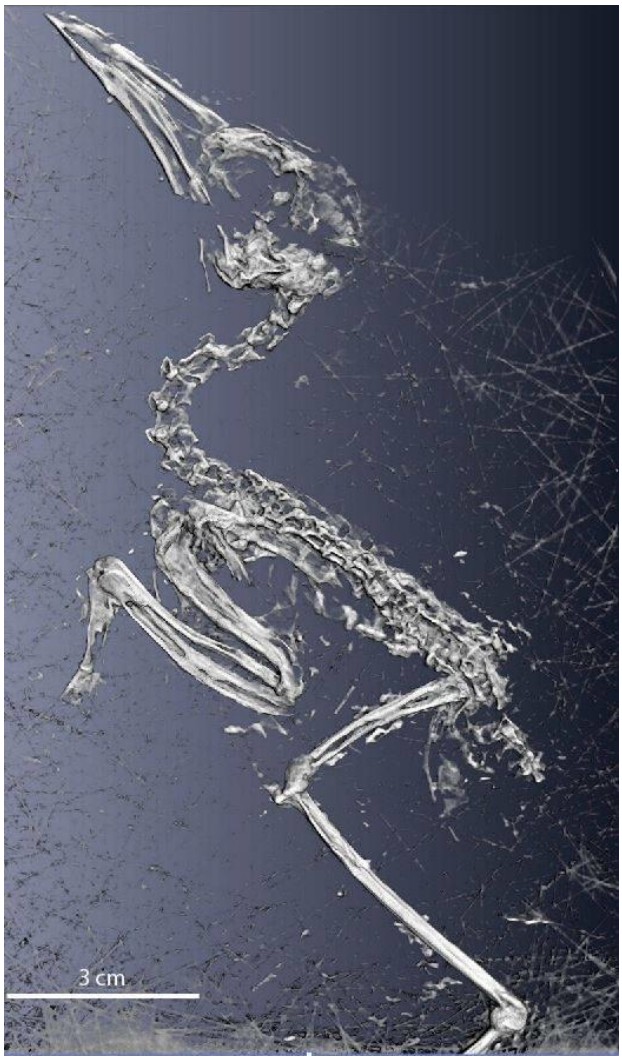

Figure 3: ***Micro CT scan of* Primozygodactylus major*, PMO 212.659 oriented in lateral view. Because of the size limitations of the CT scanner, the foot is missing in this scan.***

2.1.1 Image segmentation

A 3D model of the quadrate and os carpi radiale (see description) were created of the data obtained from the CT scan. The scan of the cranium revealed that the quadrate was three-dimensional, which made it possible to create a 3D model. The data for the os carpi radiale was collected from a different scan, which was of the pectoral and wing region (see description). When analyzing the CT data, the data were imported to Avizo fire 8.1 for 3D visualization. There are various technique to do this, but the volume rendering technique is best for CT imagery (Ni et al., 2012) . The image segmentation makes it possible to reconstruct the bone and this is done by having three planes: XY, XZ and YZ. One of the challenges that were experienced when creating the 3D model was the differentiation of bones in the orthoslice (cross-section) of the CT scan. Orthoslice is an important tool for visualizing scalar data fields defined on uniform grids, e.g. 3D images volumes ("Avizo user's manual and reference manual - Visualization sciences group," 2011).
Bones often have the same density and contrast, so assumptions must be done on their outlines, and this is done manually. It is worth noting that the software uses a linear interpolation between the manually drawn outlines, and this can create artefacts. The artefacts are created because the program needs to set values for the wanted bone, and these values are sometimes not unique and therefore the program interpret them as a part of the bone. Depressions and foramina are challenges for the digital reconstruction of the bone, and by comparing the real fossil with the 3D model, it is easy to see that the interpolation ignores small foramina and fills them, and this makes the assumption of e.g. pneumatic foramina difficult (see description). In addition, the model is reconstructed by CT-images, which also can include artefacts themselves, and this can produce errors in the final results (Ni et al., 2012).

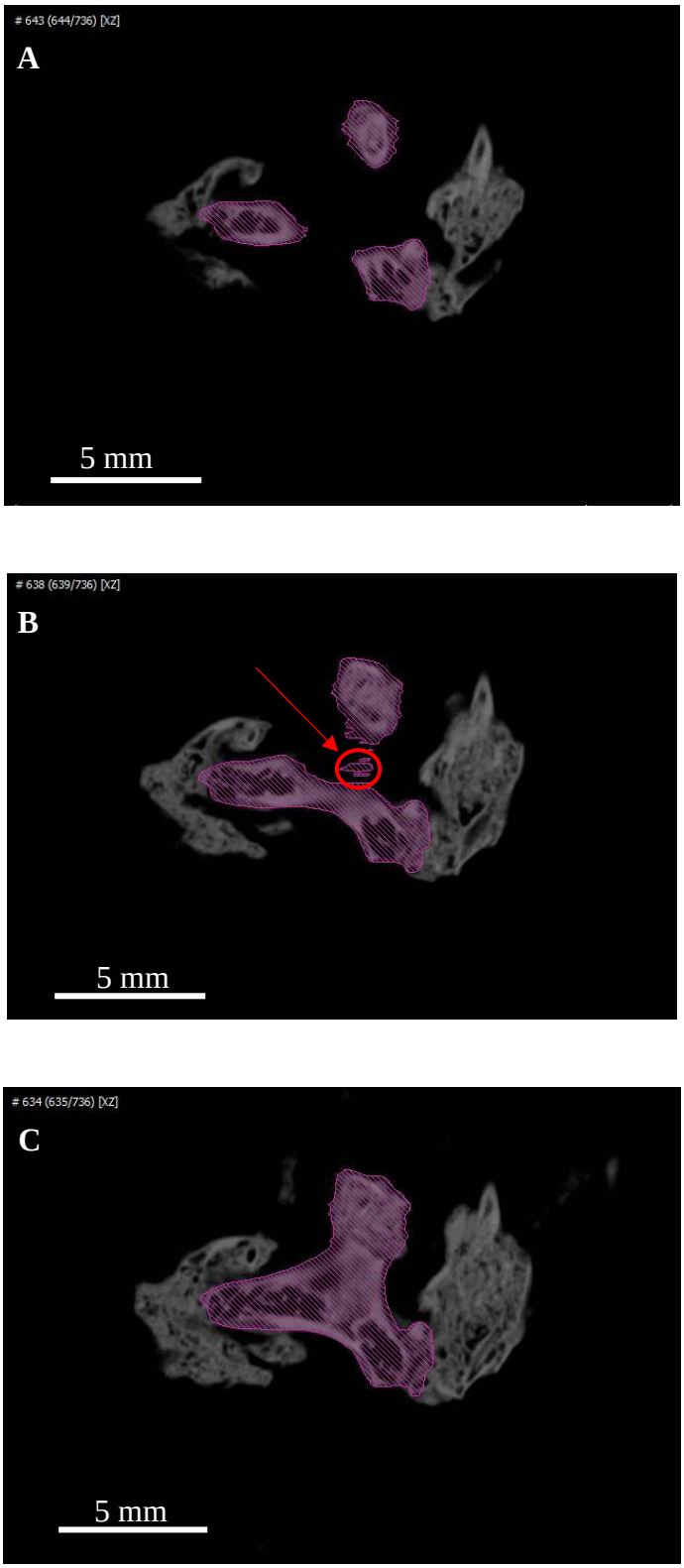

Figure 4: ***The orthoslices, A-C show different sections of the quadrate (violet) in lateromedial view. An interpolation method was used and this is a series of figures that shows how the interpolation method works. The red circle and arrow indicates an imagine artefact.***

The Figure series 4 A-C is the result of the interpolation of the quadrate. The CT data is stacked, and makes it possible to browse to data section by section. This makes it possible to manually highlight the parts that are desirable, and is done on every 5^{th}-10^{th} slice. Figure 4B shows how the interpolation can create artefacts in that all the parts of the quadrate are connected, ignoring the fact that in some regions there is actually no bone present. The program does this to make the transitions smoother, but then it can create a false image of the bone. These artefacts are most common, and can easily be removed by manual corrections. It is easy to observe some of the artefacts in Figure 5A, where the 3D model is overlying the original CT data (Figure 5B).

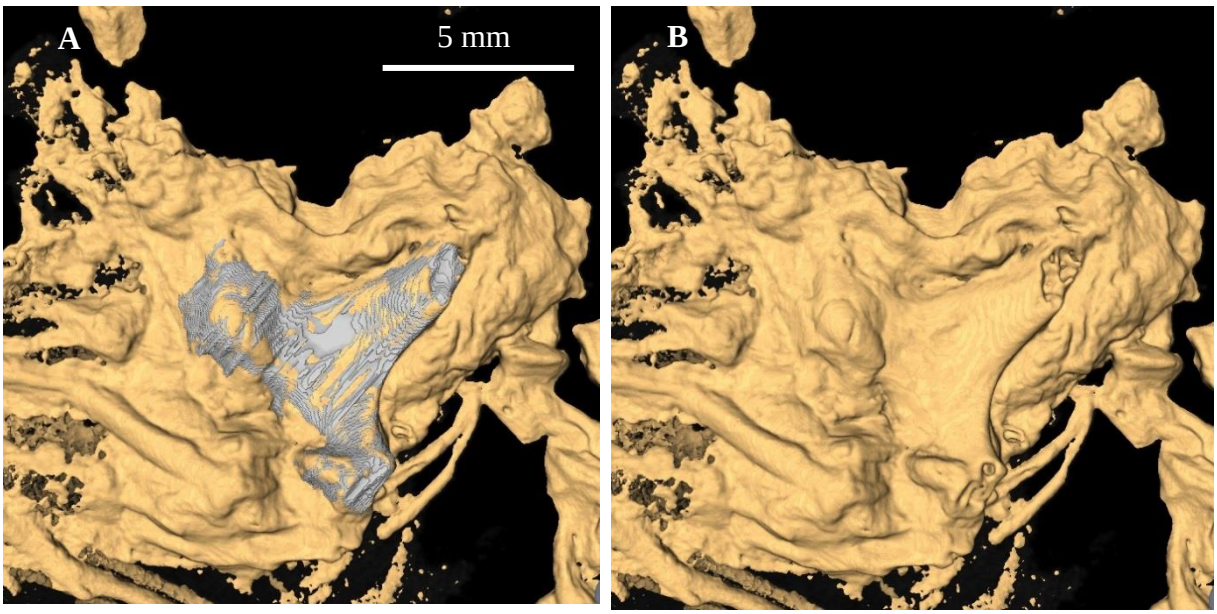

Figure 5: ***A, The 3D model of the quadrate (grey) is the extracted from the original CT data (B). B, the original CT-data. The bone is seen in lateral view.***

The majority of these artefacts can be removed by using an "islands filter" (floating objects that are surrounding the bone). After removing all the unwanted objects and artefacts, smoothing is applied to the surface to remove further noise. This is done by first smoothing all the slices, and then applying 3D volume smoothing that uses all of the three planes (XY, XZ, and ZY). When all the operations are done, the model looks like the one shown in Figure 6A. The model still contains contouring, and a final process is applied. The final result is a smooth and realistic reconstruction of the studied bone (see Figure 6B).

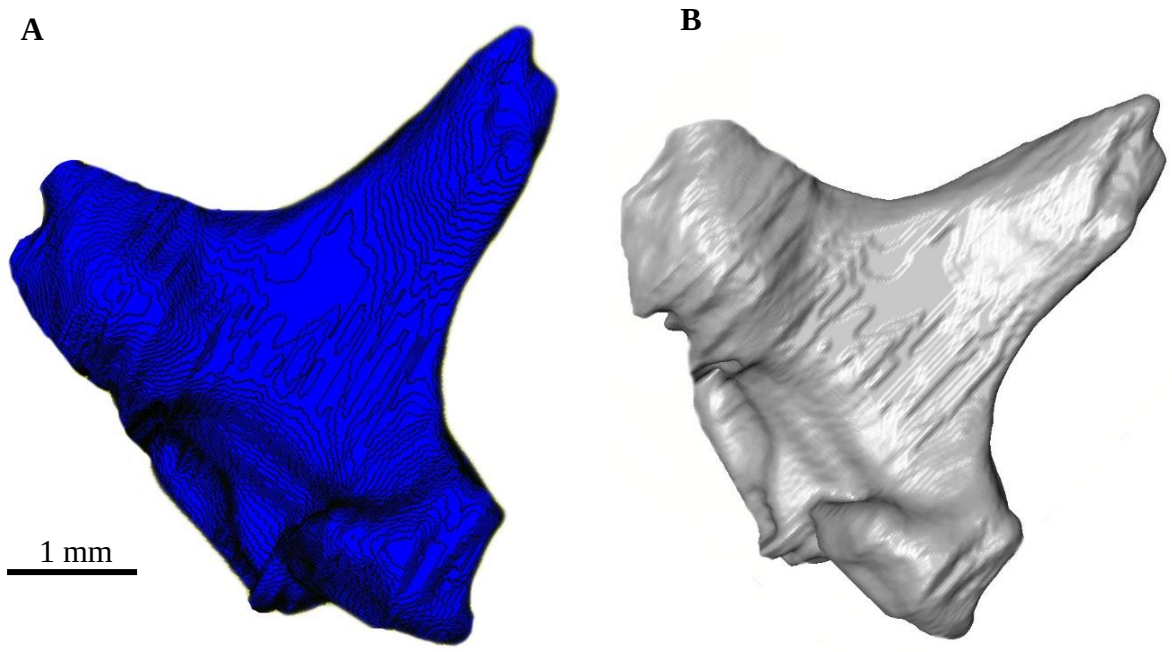

Figure 6: ***A, quadrate before the "generate surface" process and B, quadrate after the "generate surface" process. This process removes striations and contouring in the model. The quadrate is oriented in lateral view.***

Institutional Abbreviations

PMO, University of Oslo, Natural History Museum (palaeontological collection), Norway.

SMF, Forschungsinstitut Senckenberg, Frankfurt am Main, Germany.

FMNH, Field Museum of Natural History, Chicago, Illinois, USA.

USNM, National museum of Natural History, Washington, DC, USA.

WN, Walton-on-the-Naze, England.

Abbreviations used in tables and figures

acc = trochlea accessoria
acro = acromion
alu = phalanx digit alulae
ang = angular,
b = beak
c = clavicle
ccc = crista cnemialis cranialis
cd = condylus dorsalis
cdp = crista deltopectoralis
cmh = crista medialis hypotarsi
cl = crista lateralis
cm = crista medialis
cmc = carpometacarpus
cor = opening on corpus vertebrae
cr = cervical ribs
cv = condylus ventralis
d = dentary
dd = dentary depression
ecv = epicondylus ventralis
ecr = sulcus for tendon of musculus extensor carpi radialis
ect = ectethmoid
dc = depression caudomedialis
f = frontal
fam = facies articularis metacarpalis
far = facies articularis radialis
fb = foramen pneumaticum basiorbitale,
fcv = free caudal vertbrae
fdl = canal for tendon of musculus flexor digitorum longus
fem = femur
fhl = canal for tendon of musculus flexor hallucis longus
fib = fibula
h = humerus
hy = hyoid bone
ic = incisura capitis
ili = ilium
imc = processus intermetacarpalis
isc = ischium
ischio = ischiopubic fenestra
itv = fenestra intertransveraria
jug = jugal
l = lacrimale
lc = condyus mandibularis laterocaudalis
lco = left coracoid
l**exc** = lateral excavation
lig.ela = area ligament elastici
lr = left radius
luln = left ulna
m = condyles mandibularis medialis
majoris = phalanges digit majoris
mdl = mandible

mes = mesethmoid
minoris = phalanx digit minoris
mt = lateral trochlea of the medial condyle
n = nasal
nfh = nasofrontal hinge
nos = nostril
o = capitulum oticum
ocr = os carpi radiale
or = processus orbitalis
par = parietal
prem = premaxilla
prj = distoventral projection
proc.spin = processus spinosus
proc.trans. = processus transversus
pt = condyles pterygoideus
pu = pubis
q = quadrate
qj = cotyla quadratojugalis
rco = right coracoid
ruln = right ulna
s = capitulum squamosum
sc = scapula
scl = scleral ring
slc = culcus on the plantar surface of anterolateral convexity
sq = squamosal
st = sulcus tendineous
surang = surangular
tm = trochlea metatarsi III
tmt = tarsometatarsus
tt = tibiotarsus
umv = notch for tendon of musculus ulnometacarpalis ventralis
zyga.caud = zygapophysis caudalis
zyga.cran = zygapophysis cranialis

3. Description of PMO 212.659

Aves Linnaeus, 1758

Zygodactylidae Brodkorb, 1971

Primozygodactylus Mayr, 1998

Primozygodactylus major Mayr, 1998

Assigned specimens: SMF ME 1758a+b (holotypus), almost complete articulated skeleton (Mayr, 1998, tafel 16). SMF ME 799a+b, incomplete and dissociated skeletons (Mayr & Zelenkov, 2009, fig. 3).

Referred specimen: PMO 212.659, almost complete articulated skeleton lacking the right femur, tibiotarsus and tarsometatarsus (see Figure 2).

Locality and horizon: Messel near Darmstadt, Hessen, Germany; early Eocene, MP11 (Legendre & Léveque, 1997)

Diagnosis: The skeleton of PMO 212.659 is identified as a *Primozygodactylus major* due to the following trait: The tarsometatarsus is elongated and similar in length and shape as SMF ME 1758 (29.5 mm vs. 28.0 mm), but has a slightly longer tibiotarsus (44.1 mm vs. 39.0). The tibiotarsus is similar in length to SMF ME 799 (44.0 mm). The tarsometatarsus possesses a large trochlea accessoria, which is seen in all *Primozygodactylus*. The carpometacarpus is large and with the os carpalis minus reaching the large intermetacarpal process. The long and narrow nasal opening measures half of the entire beak size (15.5 mm). Ulna is distinctly longer than the tarsometatarsus (32.7 vs. 29.5). PMO 212.659 exhibits a massive acromion, which is long and is a diagnostic trait for *P.major*, within the genus. The measurements of the major limbs are similar to the holotype and almost identical to SMF ME 799.

Mesurements. – see Table 1,2 and 3.

Table 1: **Total length (in mm) of cranial foramina and cranial bones of *Primozygodactylus major* Mayr, 1998, and Mayr and Zelenkov, 2009. Abbreviations:** b, **beak;** nos, **nostril;** mdl, **Mandible;** or, **orbit;** q, **quadrate.**

	B	**NOS**	**MDL**	**Q**	**OR**
PMO 212. 659	27.8	15.5	~44.0	5.5	9.5
SMF ME 1758	?	12.9	~42.0	?	~10.0
SMF ME 799	?	?	?	?	?

Table 2: **Total length (left/right in mm) of the pectoral and wing bones of *Primozygodactylus major* Mayr, 1998, and Mayr and Zelenkov, 2009. Abbreviations:** c, **clavicle;** co, **coracoid;** cmc, **carpometacarpus;** h, **humerus;** r, **radius;** sc, **scapula;** uln, **ulna.**

	H	**R**	**ULN**	**CMC**	**SC**	**CO**	**C**
PMO 212. 659	28.0/-	~29.7/-	32.7/~23.8	14.0/-	~29.9/-	~18.5/~18.1	~16.0/-
SMF ME 1758	~28.4/-	~27.9/-	~31.1/-	~12.0/-	?	~18.6/-	?
SMF ME 799	-/29.0	?	-/~33.5	-/-	?	?	?

Table 3: **Total length (left/right in mm) of the hind limbs of the species Primozygodactylus major Mayr, 1998, and Mayr and Zelenkov, 2009. Abbreviations:** fem, **femur;** tmt, **tarsometatarsus;** tt, **tibiotarsus.**

	FEM	**TT**	**TMT**
PMO 212. 659	27.5/-	44.1/-	29.5/-
SMF ME 1758	24.6/-	39.0/39.8	28.0/-
SMF ME 799	-/-	42.8/44.0	-/-

3.1 Cranial skeleton

The cranium of PMO 212.659 is in good condition (see Figure 7), but shows some crushing and has a small crack, which goes from the underside of the mandible towards the caudal end of the frontal. It is worth noting that deformation of the skull is quite common in small bird fossils from Messel. The cranium is oriented in a left lateral view.

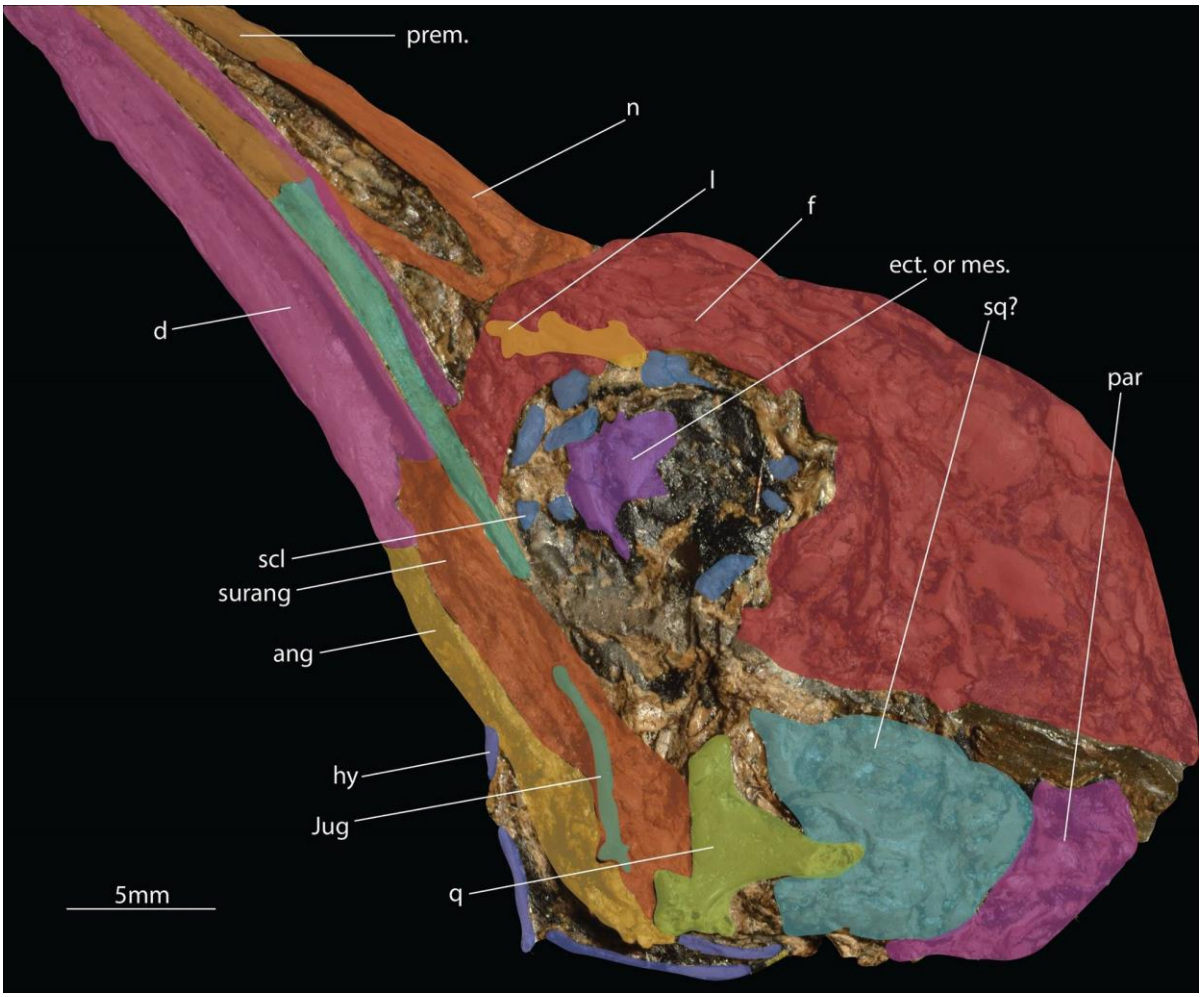

*Figure 7**: Interpretation of the caudal portion of the skull of* **Primozygodactylus major***, PMO 212.659, in left lateral view.* ***Abbreviations:*** *ang,* ***surangular;*** *d,* ***dentary;*** *ect,* ***ectethmoid;*** *f,* ***frontal;*** *hy,* ***hyoid bone;*** *jug,* ***jugal;*** *l,* ***lacrimal;*** *mes,* ***mesethmoid;*** *n,* ***nasal;*** *prem,* ***premaxilla;*** *q,* ***quadrate;*** *scl,* ***scleral ring;*** *sq,* ***squamosal;*** *surang,* ***surangular.***

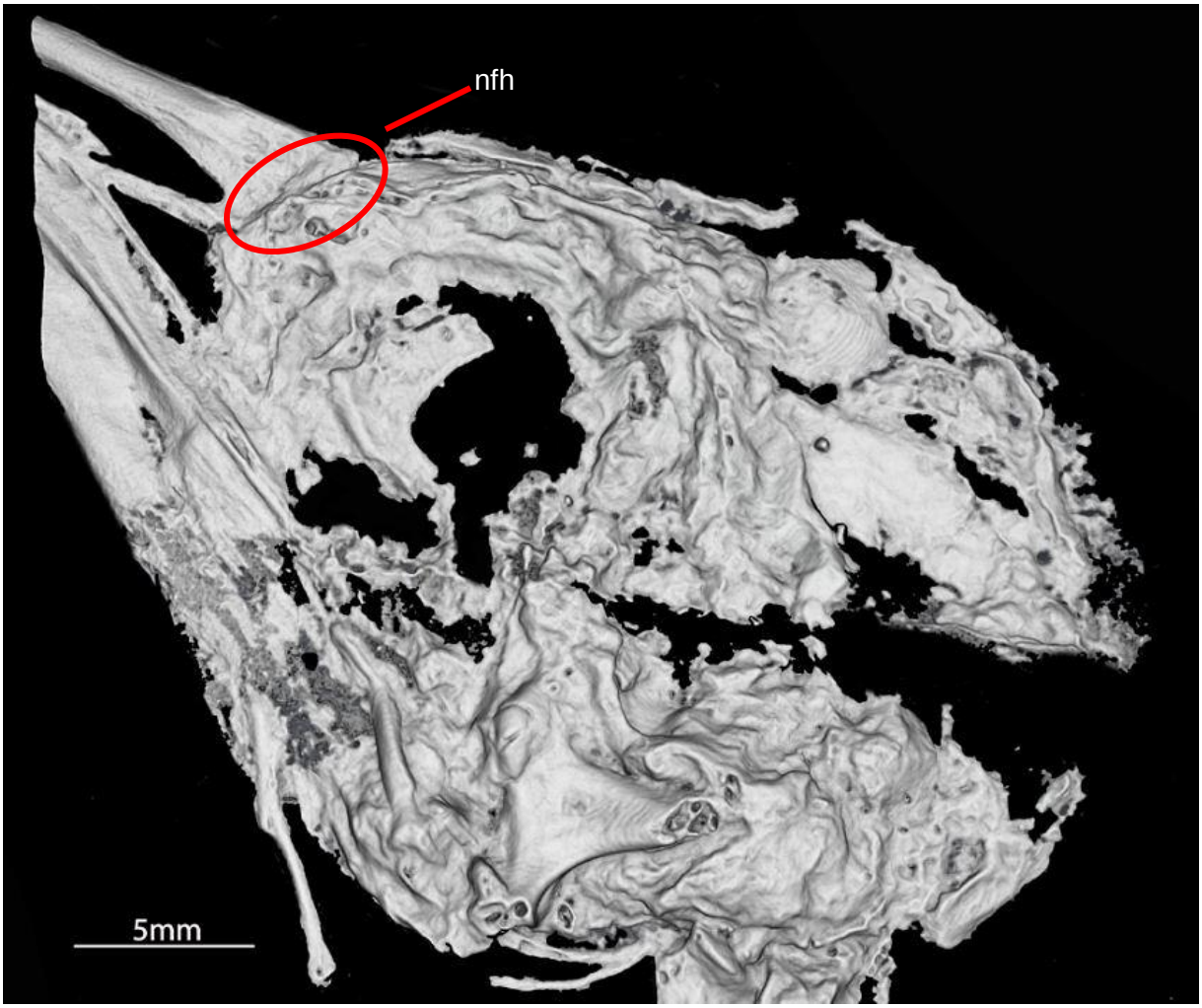

Figure 8: ***Micro CT scan of the caudal portion of the skull of* Primozygodactylus major*, PMO 212.659, in left-lateral view. Abbreviation:*** *nfh,* ***nasofrontal hinge.***

The skull bones of adult birds are fully fused, and the sutures between the frontal, partial, squamosal and the other skull bones are therefore not visible (Liem, 2001). Taken this into account, an approximation has been done for some of the skull bones. Figure 7 highlights the major bones in the cranium. The skull bones that have not been mentioned are too crushed for detailed studies.

The beak is long and narrows towards the distal end. The premaxilla is crushed and broken in this area, but is preserved good enough to discern its outline. The specimen has a well preserved nostril, which is similar to that of the holotype in its shape (SMF-ME 1758). The nostril is large and has a triangular shape, widening caudally, measuring about half (15.5

mm) of the total length of the beak. The antorbital fenestra is relatively large, and has a triangular shape. The lacrimale is for the first time preserved in a *Primozygodactylus* specimen, but is unfortunately crushed, and no details can be observed. The nasofrontal hinge is well developed and can easily be seen in the micro-CT scan of the cranium (see Figure 8). Scleral ossicles can be observed in the orbital opening, but only 10 scleral ossicles are clearly discernible. Because some are shifted out of position, it is difficult to ascertain their full original number. Earlier reconstructions of the sclerotic ring suggest that the sclerotic ring consists of 15 plates (Mayr, 1998), which indicates that the present specimen (PMO 212.659) lacks some of the scleral ossicles. The identification of the bone in the orbit is uncertain, but is considered to be either the ectethmoid or the mesethmoid (see Figure 7).

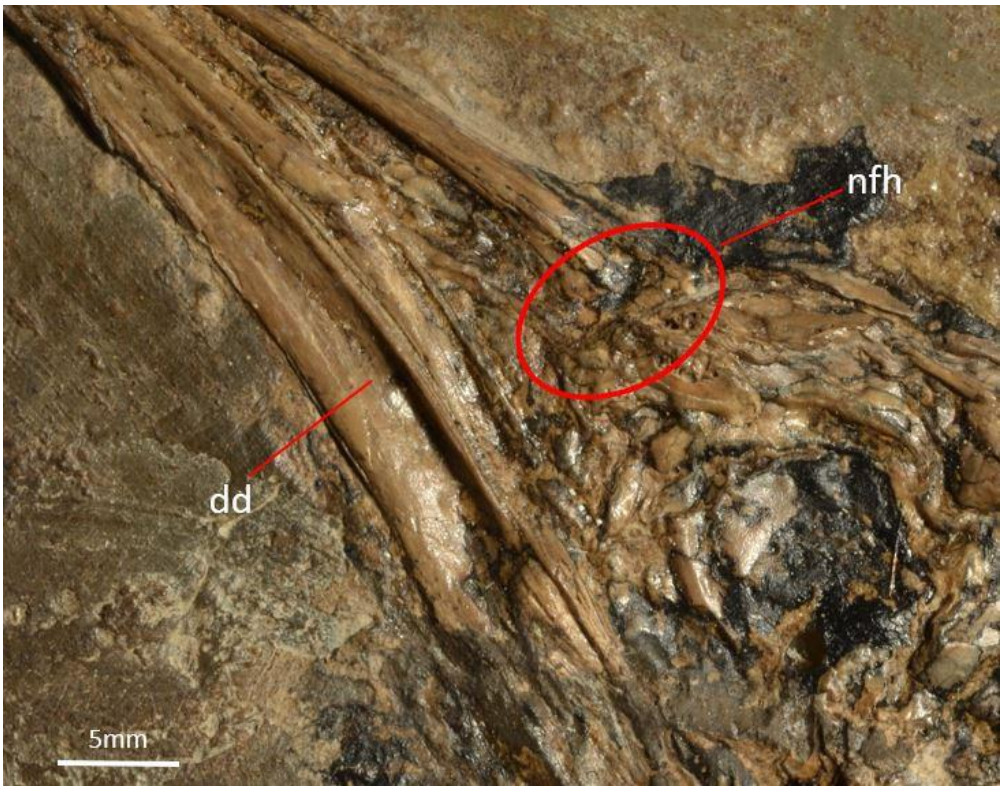

Figure 9: ***The beak and mandibular of* Primozygdactylus major*, PMO 212.659 in lateral view. The red circle indicates the nasofrontal hinge. Abbreviation:*** *dd,* ***dentary depression;*** *nfh,* ***nasofrontal hinge.***

The proximal end of the mandibula is broken, but the outline and impression of the bone allow a reconstruction of the entire bone and no mandibular fenestra is visible, which is in accordance with previously described fossils of *Primozygodactylus* (Mayr, 1998). A

mandibular fenestra is common in the Passeriformes. The dentary has a depression, which does not seem to be an artefact of compaction (see Figure 9). This depression can also be observed in plate B and in the holotype specimen of *Eozygodactylus americanus* (USNM 299821) (Weidig, 2010). The angular and surangular are crushed and make the outline of the bones difficult (see Figure 7). The maxilla, quadratojugale and the jugale are partially preserved. The proximal end of the quadratojugale is well-preserved and shows the condylus quadraticus.

The left quadrate of PMO 212.659 is preserved in lateral view (see Figure 10). The CT-scan of the cranium revealed that the bone was three-dimensionally preserved, and almost complete (see Figure 11). A 3D-model was created to study the features hidden by the matrix. This is the first time, a quadrate of the Zygodactylidae can be studied in detail from all views. It is just in the past few years that detail studies of extant and fossil bird quadrate have been done. Most of the studies are done by Elzanowski, (Elzanowski, 2013; Elzanowski & Boles, 2012, 2015; Elzanowski & Stidham, 2010, 2011) who has made great progress in describing the morphology of quadrates variety in the different bird taxa.

The relative size and shape of the quadrate in PMO 212.659 is similar to small-medium sized birds (e.g. *Corvus* and *Coccothraustes*), and closely resembles that of the Piciformes, Upupiformes and Passeriformes (Samejima & Otsuka 1987, fig. 1B).

Judging from the reconstructed 3D model of the micro CT-scan data (see Figure 11), the orbital process is short and stout in PMO 212.659, but looks to be crushed in the distal end, making it difficult to give an exact length of this process (see Figure 11B). However, the length of the orbital process is similar to *Eozygodactylus americanus* (USNM 299821), which was described by Weidig (2010). The orbital process in PMO 212.659 and USNM 299821) is directed rostrodorsally. Plate B and USNM 299821, both show slight medially tilt of the orbital process, which suggest a rostromedial protrusion, which is common in Passeriformes and Piciformes.

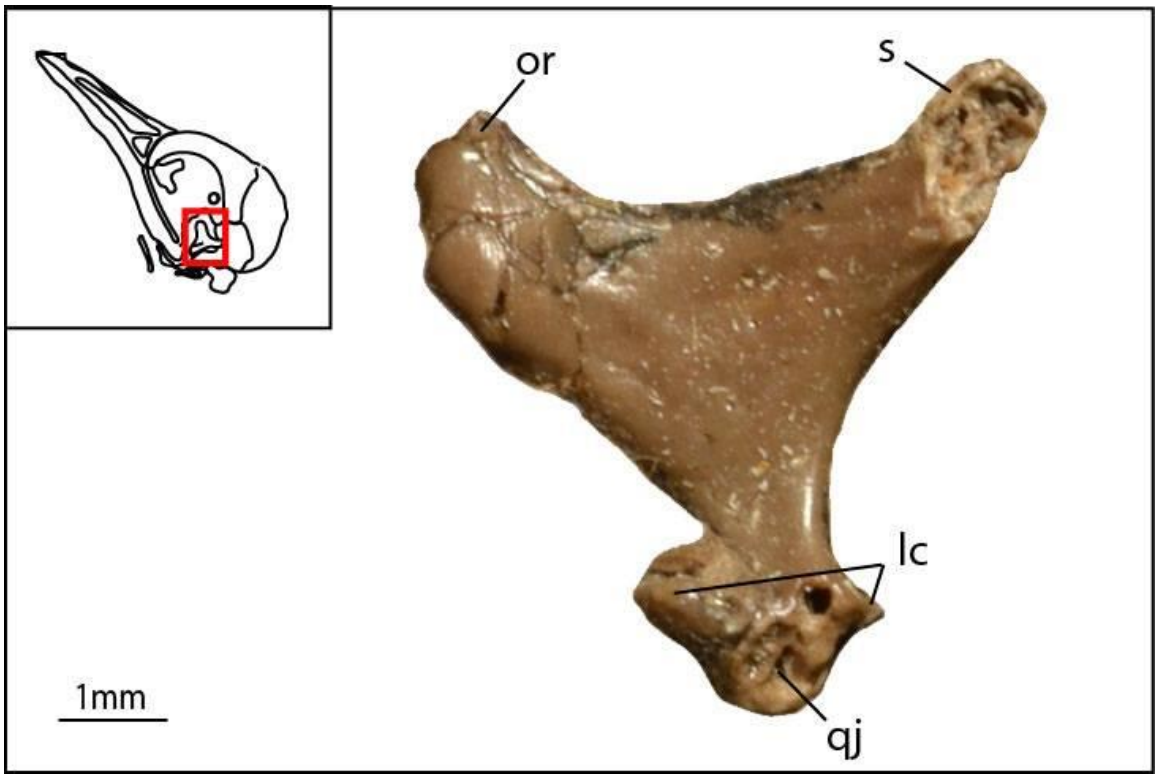

Figure 10: ***Photograph of the left quadrate of*** **Primozygodactylus major*****, PMO 212.659. The bone is seen in lateral view. Abbreviations:*** *lc****, condylus mandibularis laterocaudalis;*** *or****, processus orbitalis;*** *pt****, condylus pterygoideus;*** *qj****, cotyla quadratojugalis;*** *s****, capitulum squamosum.***

The medial condyle protrudes ventrocaudally and is short, which is similar to the quadrate of the holotype of *P. major* (SMF-ME 1758a) (Mayr, 1998). The medial condyle is large and protrudes further ventrally than the lateral condyle. In ventral view both the lateral and medial condyle resemble those of the Passeriformes and Piciformes (see Figure 11F). The lateral condyle seems to be a bit more compacted and not as laterally projected as in the Passeriformes. However, in caudal view the lateral condyle is remarkably similar to the Passeriformes (e.g. *Coccothraust* and *Corvus*) (see Figure 11C). The cotyla quadratojugalis is not clearly visible in the fossil, and is only visible as a depression in the 3D model (see Figure 10 and 11A). The depression appears to be shallow and might be a trait for *Primozygodactylus major*, and is seen in many higher land birds (Piciformes, Psittaciformes and Coraciiformes), but not in the Passeriformes (Samejima & Otsuka 1987: fig. 2). The capitulum oticum and squamosum are facets shaped, and are best viewed in caudal aspect. The capitulum oticum is large and wide, and has a well-developed medially protrusion. This protrusion seems to be larger than that of the Passeriformes (see Figure 11C) and similar to

the *Upupa epops*, which was described by Elzanowski and Boles (2015), but in *P. major* (PMO 212.659) it does not exhibit the hook-like shape (Elzanowski & Boles, 2015, fig. 1B). The size proportion of the capitulum oticum and capitulum squamosum is similar to the Passeriformes, and there is a slight slope from the capitulum squamosum to the capitulum oticum, with the distance between them being quite large.

The depression that can be seen in caudal view is identified as the depressio caudalmedialis, but could also be the foramen pneumaticum rostromedialis. In caudal view the crista caudalis and crista tympanica are quite well-developed. The condylus pterygoideus is preserved as a facet shaped articulation surface, but it is uncertain (see Figure 11B). There is a depression observed at the base of the capitulum, it is uncertain however, if this is the foramen pneumaticum caudomediale (see Figure 11B). The position of the putative pneumatic foramen is similar to the Passeriformes, whereas other birds like the Coraciiformes have it situated higher up on the capitulum squamosum (Samejima & Otsuka, 1987). The quadrate is preserved in plate B as well, but is unfortunately not well enough preserved to be studied only on the image alone. However, the assumed orbital process has a slightly rostromedial protrusion, which similar to PMO 212.659.

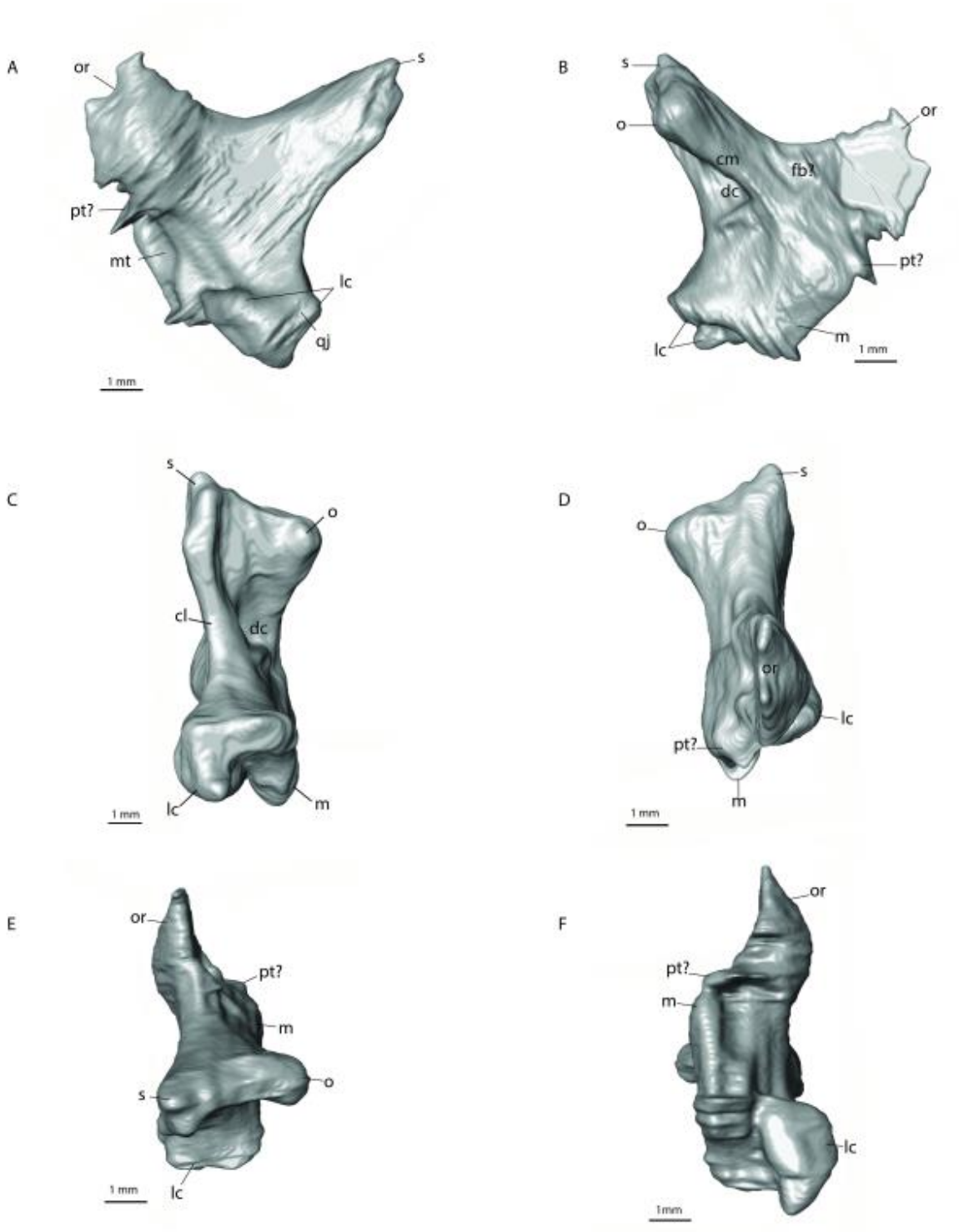

Figure 11: ***3D reconstruction of the quadrate of*** **Primozygodatylus major, PMO 212.659** ***in (A) lateral view, (B) medial view, (C) caudal view, (D) rostral view, (E) dorsal view and (F) ventral view. Abbreviations:*** *cl,* ***crista lateralis;*** *cm,* ***crista medialis;*** *dc,* ***depressio caudomedialis;*** *fb,* ***foramen pneumaticum basiorbitale;*** *lc,* ***condylus mandibularis laterocaudalis;*** *m,* ***condyles mandibularis medialis;*** *mt,* ***lateral trochlea of the medial condyle;*** *o,* ***capitulum octicum;*** *or,* ***processus orbitalis;*** *pt,* ***condylus pterygoideus;*** *qj,* ***cotyla quadratojugalis;*** *s,* ***capitulum squamosum.***

Fragments of the hyobranchial apparatus are preserved (see Figure 7 & 8), but not many details can be observed. The left ceratobranchiale seems to be split, but is more or less intact and both of the epibranchialia are present. The ceratobranchialia and the epibranchialia have approximately the same length, this is probably due to the fragmentation of the ceratobranchiale, which in Passeriformes has twice the relative length (Manegold, 2008) and should be seen in PMO 212.659.

3.2 Postcranial skeleton

3.2.1 Vertebral column

Nine cervical vertebrae and eight thoracic vertebrae are visible in the fossil. Based on information from the holotype of *P.major* (SMF-ME 1758) and the other species of the genus, it has been determined that *Primozygodactylus* has 19 pre-synsacral vertebrae, the same number as in the Passeriformes and Piciformes (Mayr, 1998). Here, only 17 vertebrae can be discerned, but the atlas and axis are not visible, which explains the lower vertebral count. The 4th cervical vertebra is orientated in a dorsal aspect, and this is more or less consistent in all of the cervical vertebrae. The 11th cervical vertebra has a slightly more lateral orientation, which indicates that the neck is twisted. Almost all the cervical vertebrae possess cranial and caudal zygapophyses and cervical ribs. Mayr (1998) mentions that specimen SMF-ME 1758 has a wide dorsoventral "bony bridge" between the processus transversus and the processus articularis caudalis of the 3rd and 4th cervical vertebrae. This connection leaves a small opening to the corpus vertebrae, which is similar to the Passeriformes and Piciformes (Mayr, 1998). The 4th vertebra in specimen PMO 212.659 has a small opening, which corresponds with that of SMF-ME 1758 (see Figure 12). Unfortunately the 3rd vertebra is too crushed to observe this feature. The area ligamenti elastici is clearly visible in the 6th and 7th cervical vertebrae, and is similar to that of the *Primozygodactylus* specimen described by Mayr (1998) (see Figure 12). This depression is found in Passeriformes and Coraciiformes (Mayr, 1998).

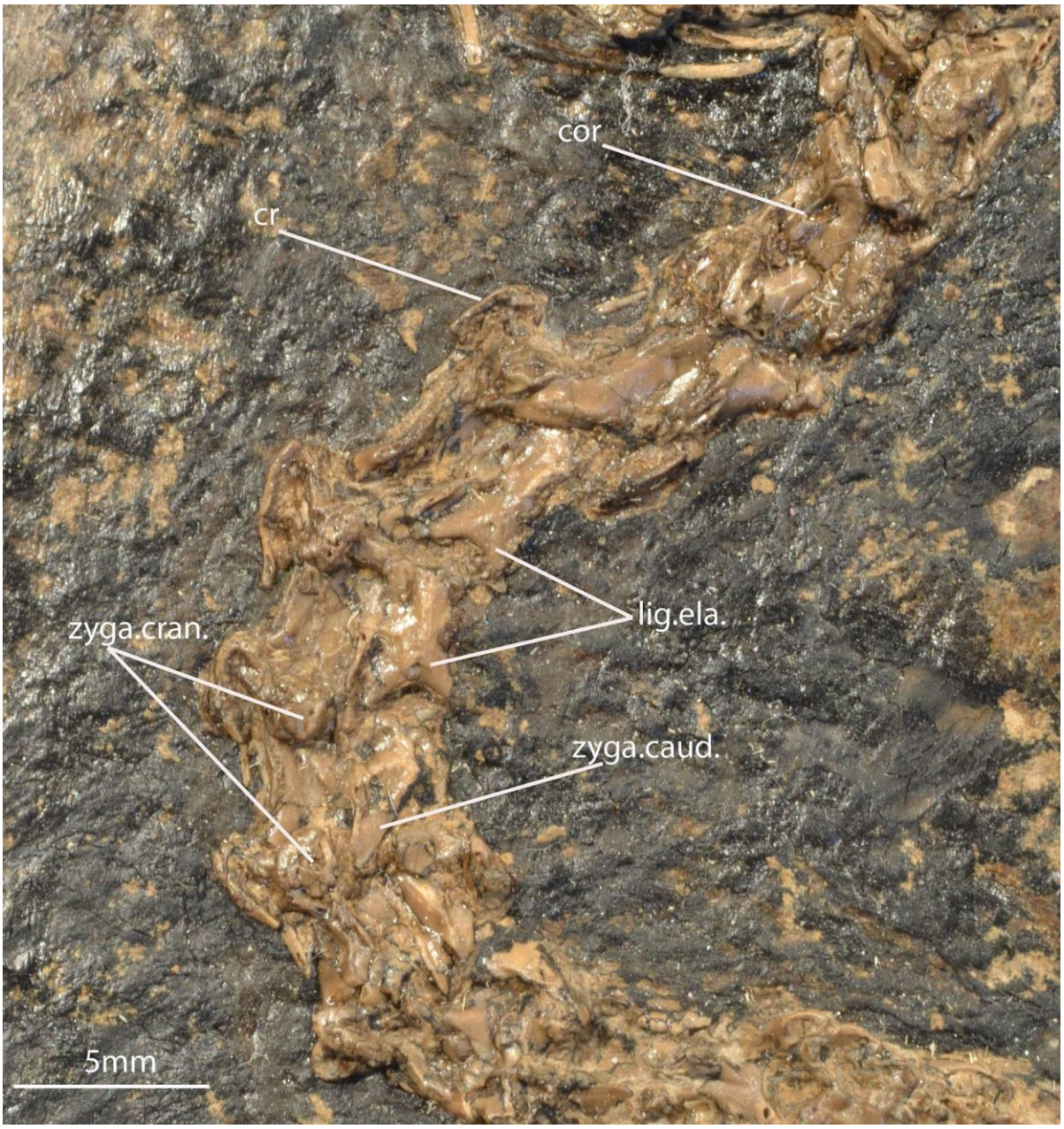

*Figure 12**: Photograph of* **Primozygodactylus major** ***PMO 212.659, the cervical vertebrae are exposed in dorsal view. Abbreviations:*** *cor,* ***opening on the corpus vertebrae;*** *cr,* ***cervical rib;*** *lig.ela,* ***area ligament elastici;*** *zyga.caud.,* ***zygapophysis caudalis;*** *zyga.cran.,* ***zygapophysis cranialis.***

The 1st thoracic vertebra is hard to see due to crushing, but the outline of it can be seen between the 2nd thoracic and 11th cervical vertebrae. The thoracic vertebrae exhibit fenestra intertransversaria, processus spinosus and the most caudal thoracic vertebrae have lateral excavations. The lateral excavations are also found in the holotype (SMF ME 1758a), but is better preserved in this specimen (PMO 212.659) (see Figure 13A and B). This feature is seen in other birds, like basal Galliformes (*Paraortygoides*) (Dyke & Gulas, 2002)

and in a number of Mesozoic non-neornithines (Chiappe, 2002; Norell & Clarke, 2001) and other neornithine birds, although the distribution is highly variable (Dyke & Gulas, 2002). The vertebral spines in PMO 212.659 and is similar other described *Primozygodactylus* (Mayr, 1998). The thoracic vertebra possesses excellent three-dimension preservation of processus transversi in lateral view.

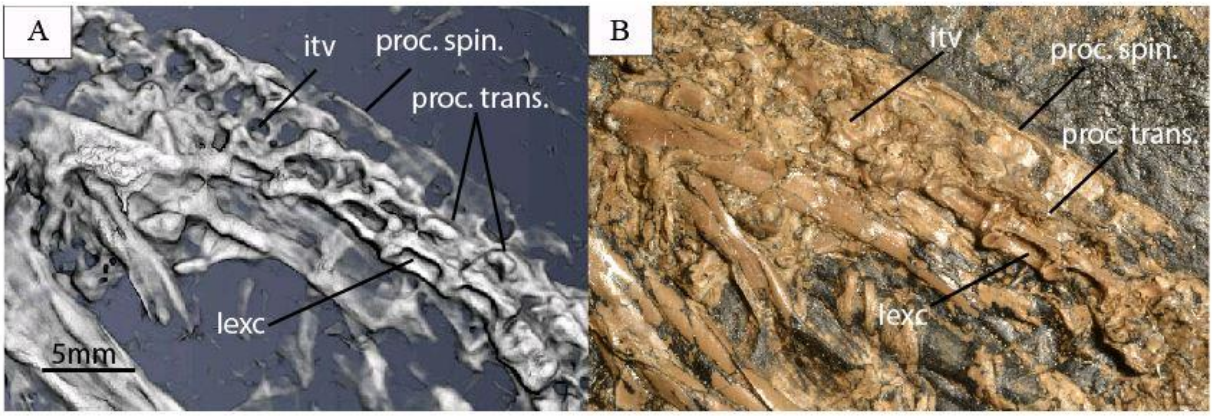

Figure 13: ***A, CT scan of* Primozygodactylus major*, PMO 212.659 in the lateral view; B, Photograph of* Primozygodactylus major *PMO 212.659, the thoracic vertebrae are orientated in the lateral view. Abbreviations:*** *lexc,* ***lateral excavation,*** *itv,* ***fenestra intertransveraria;*** *proc.spin,* ***processus spinosus;*** *proc.trans,* ***processus transversus.***

Several thoracic and sternal ribs are preserved. The most caudal ribs lie in pairs and show well-developed, processus uncinati, whose shape is similar to that in the Passeriformes and Piciformes.

The sternum is highly fragmentary in PMO 212.659, which makes is it difficult to observe any details. The counter slab, however, shows a nearly complete sternum, but due to the quality of the photograph (the only available source of observation) no further details can be discerned.

3.2.2 Shoulder girdle and wing

The left and right coracoids are preserved in lateral and medial view, respective (see Figure 14). A part of the omal extremity of the left coracoid is obscured by the left scapula, and the sternal extremity is only preserved as an impression. However, the impression has a clear outline and the shape of the processus lateralis can be observed. This process is relatively long compared to the Piciformes and Passeriformes (Mayr, 1998), the process has already

been observed in another specimen, SMF-ME 799b (Mayr & Zelenkov, 2009). The right coracoid is obscured by the left humerus, so that the middle part is completely covered and the sternal extremity is too badly preserved to see any details. The processus acrocoracoideus, however, is preserved on the omal extremity. The process is similar to that of specimen SMF-ME 799b, and is preserved in the dorsal view (Mayr & Zelenkov, 2009). In *Primozygodactylus*, the processus acrocoracoideus is shorter and stouter than in all the other genera in the Zygodactylidae. Another feature found on the left coracoid is the facies articularis claviculae, which is visible in the medial aspect (Mayr, 1998; Mayr & Zelenkov, 2009).

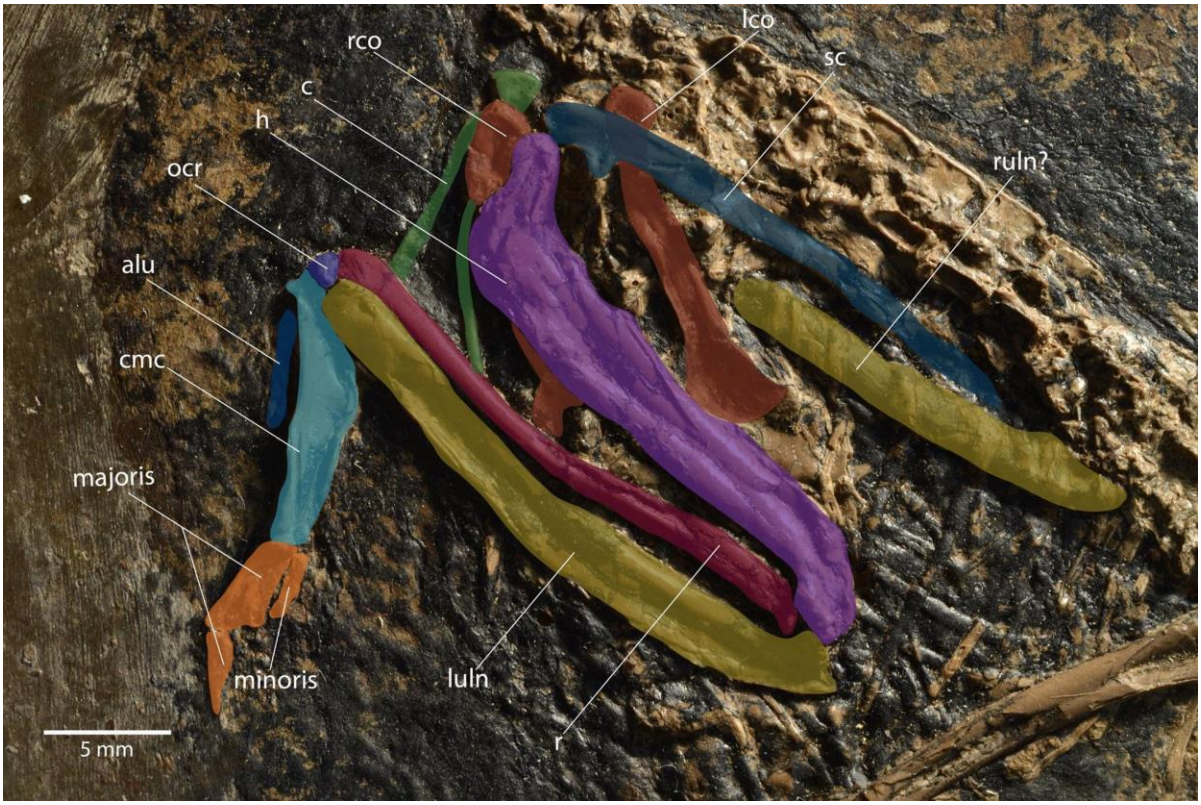

*Figure 14**: Interpretation of the pectoral girdle and left/right wing of* **Primozygodactylus major** ***PMO 212.659, in lateral view. Abbreviations:*** *alu,* ***phalanx digit alulae;*** *c,* ***clavicle;*** *cmc,* ***carpometacarpus;*** *h,* ***humerus;*** *lco,* ***left coracoid;*** *luln,* ***left ulna;*** *majoris,* ***phalanges digit majoris;*** *minoris,* ***phalanx digit minoris;*** *r,* ***radius;*** *rco,* ***right coracoid;*** *ruln,* ***right ulna;*** *sc,* ***scapula.***

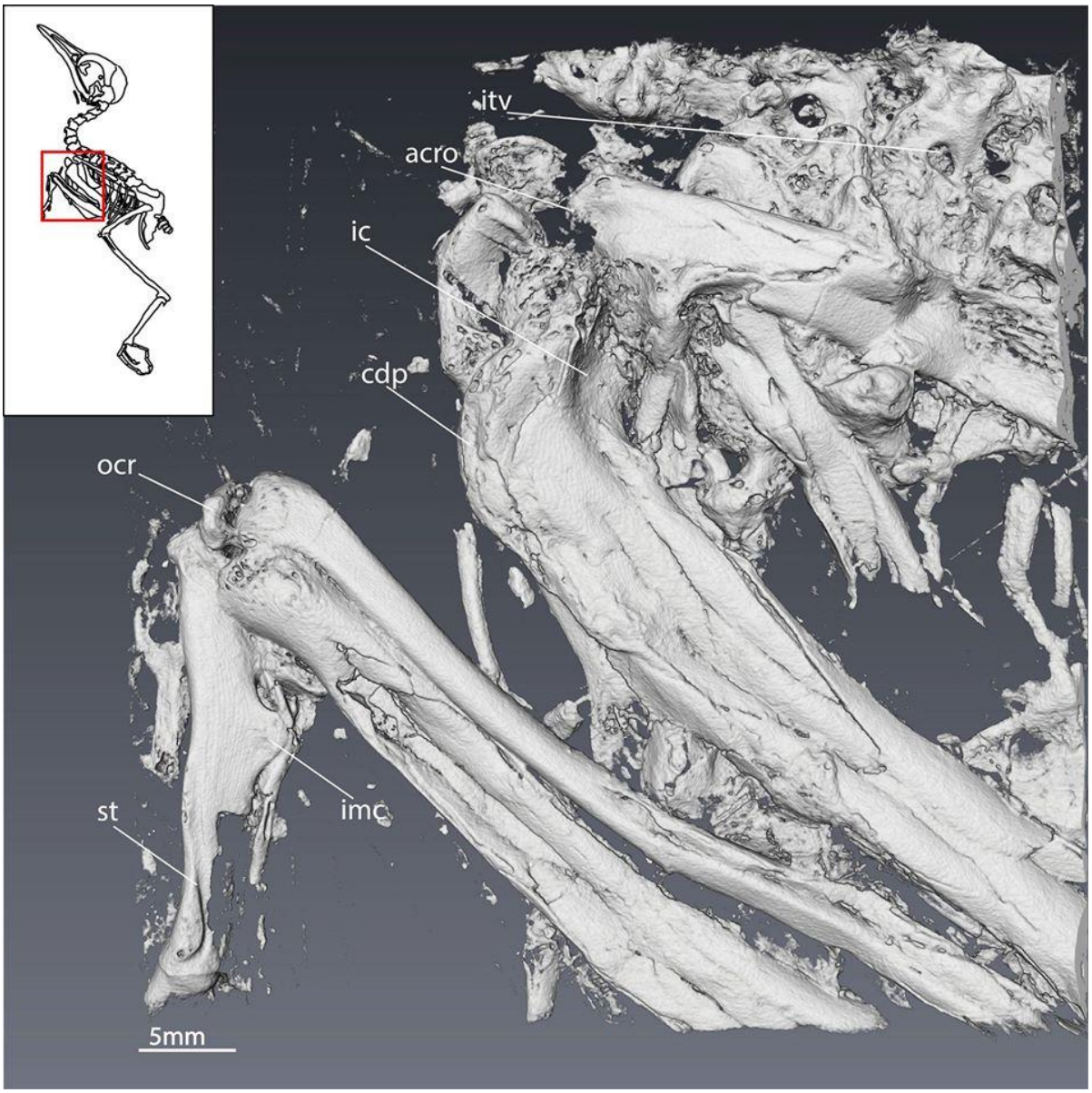

Figure 15: ***Micro CT scan image of the pectoral region and left wing. Abbreviations:*** *acro****, acromion;*** *cdp****, crista deltopectoralis;*** *itv****, fenestra intertransversaria;*** *ic****, incisura capitis;*** *imc****, intermetacarpal process;*** *ocr****, os carpi radiale;*** *st.****, sulcus tendineous.***

There are small fragmentary bones, which are located left of the humerus and are identified as fragments of the furcula. The left scapus claviculae shows a process that seems to be the apophysis, which indicates that the furcula is flipped upside down, but this is uncertain. The outline of the assumed furcula can be seen in Figure 14.

The cranial end of the left scapula is well preserved, but only as an impression on the caudal end. The scapula in this specimen (PMO 212.659) is elongated, which is a distinct

feature for this species and shows a long and massive acromion on the cranial end. These features are similar to that of the previously described *P.major* (SMF-ME 1758 and SMF-ME 799) (Mayr, 1998; Mayr & Zelenkov, 2009) (see Figure 15). The left humerus of PMO 212.659 is visible in lateral view, and is similar in size and length to *P.major* (see Table 2). The crista deltopectoralis is well visible in the CT-scan image (see Figure 15). The caput humeri are similar to that of *Zygodactylus* (Mayr 2008), and the incisura capitis is wide. The distal end of the humerus is crushed, but the processus supracondylaris dorsalis seems to be present. The right humerus is not preserved in PMO 212.659, whereas pectoral and thoracic region is covering the bone. The right humerus, however, is visible in plate B, and is well-preserved in the distal end. It is preserved in cranial view and shows great similarities to *P. danielsi* (WN 88583A and SMF-ME 2522) specimens, (Mayr, 1998, Abb. 25B and C) in the arrangement and size of the condylus dorsalis and ventralis (see Figure 16). It is uncertain if the epicondylus ventralis is preserved, but if it is it seems to be larger than that of the two other *P.danielsi* (Mayr, 1998) (see Figure 16).

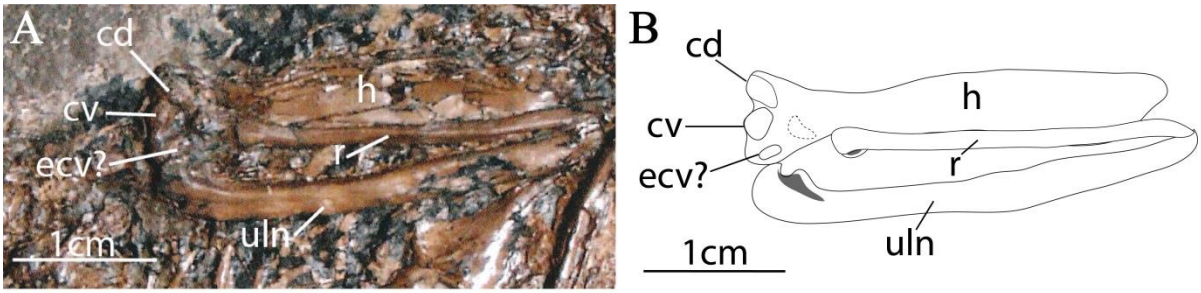

Figure 16: ***A, photograph of* Primozygodactylus major*, plate B. B, line drawing of plate B, showing the right humerus in cranial view. Abbreviations:*** *cd,* ***condyles dorsalis;*** *cv,* ***condyles ventralis;*** *ecv,* ***epicondylus ventralis;*** *h,* ***humerus;*** *r,* ***radius;*** *uln,* ***ulna.***

The left ulna and radius are preserved in PMO 212.659, but both suffer from crushing. They are both best preserved in the distal end (see Figure 15). In plate B the right ulna and radius is preserved, which is also preserved as an outline in PMO 212.659 (see Figure 14). The radius and ulna are well articulated with the os carpi radiale.

The os carpi radiale of PMO 212.659 is only partly preserved, and this makes it hard to concern some details, since a large part is missing (see Figure 17D). The details that can be seen are a wide and shallow sulcus for the tendon of musculus ulnometacarpalis ventralis, and the sulcus for tendon of musculus extensor carpi radialis (see Figures 17 & 18). The narrow sulcus for the tendon of musculus extensor longus alulae is absent, which is similar to the condition in *Z. luberonsis* (Mayr, 2014).

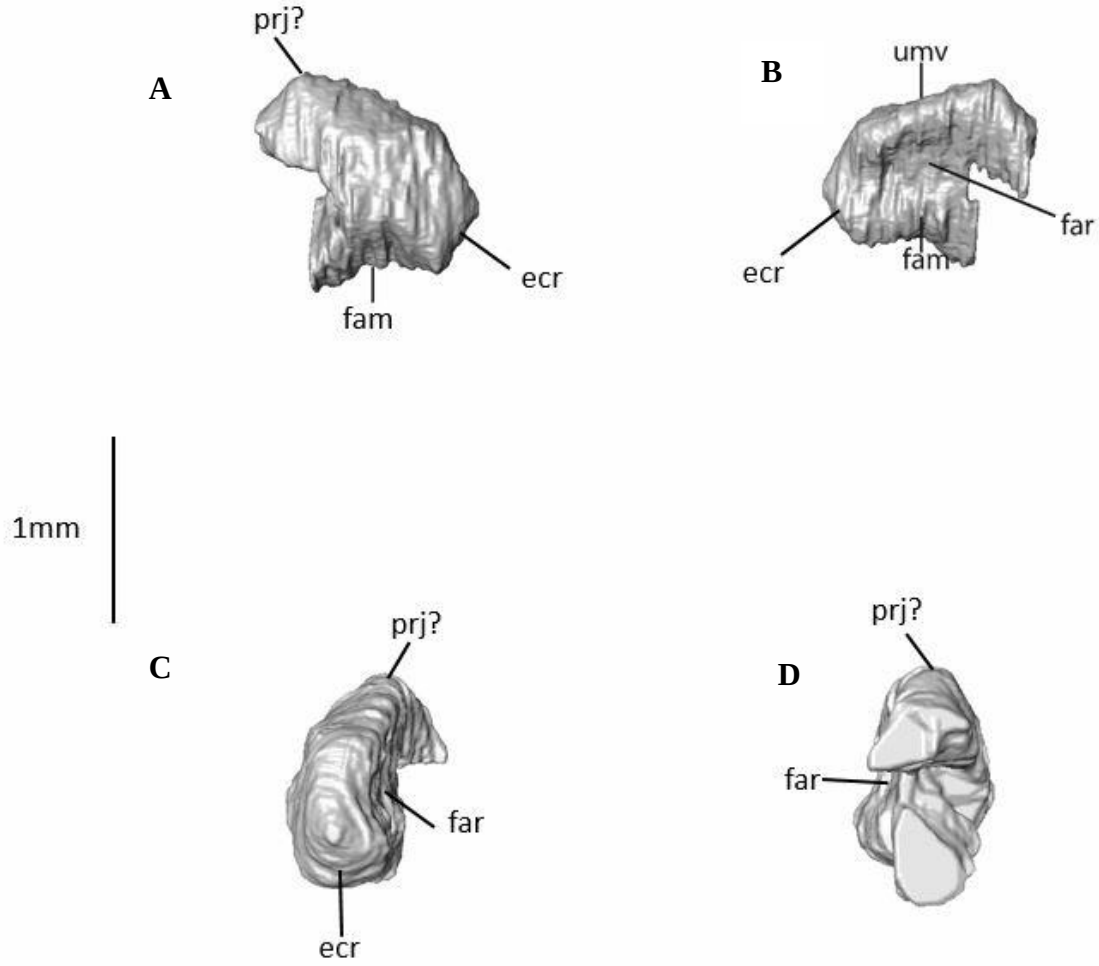

Figure 17: ***3D model of left os carpi radiale of*** **Primozygodactylus major,** ***PMO 212.659. A cranial view, B caudal view, C dorsal, and D ventral view. Abbreviations:*** *ecr,* ***sulcus for tendon of musculus extensor carpi radialis;*** *fam,* ***facies articularis metacarpalis;*** *far,* ***facies articularis radialis;*** *prj,* ***distoventral projection;*** *umv,* ***notch for tendon of musculus ulnometacarpalis ventralis.***

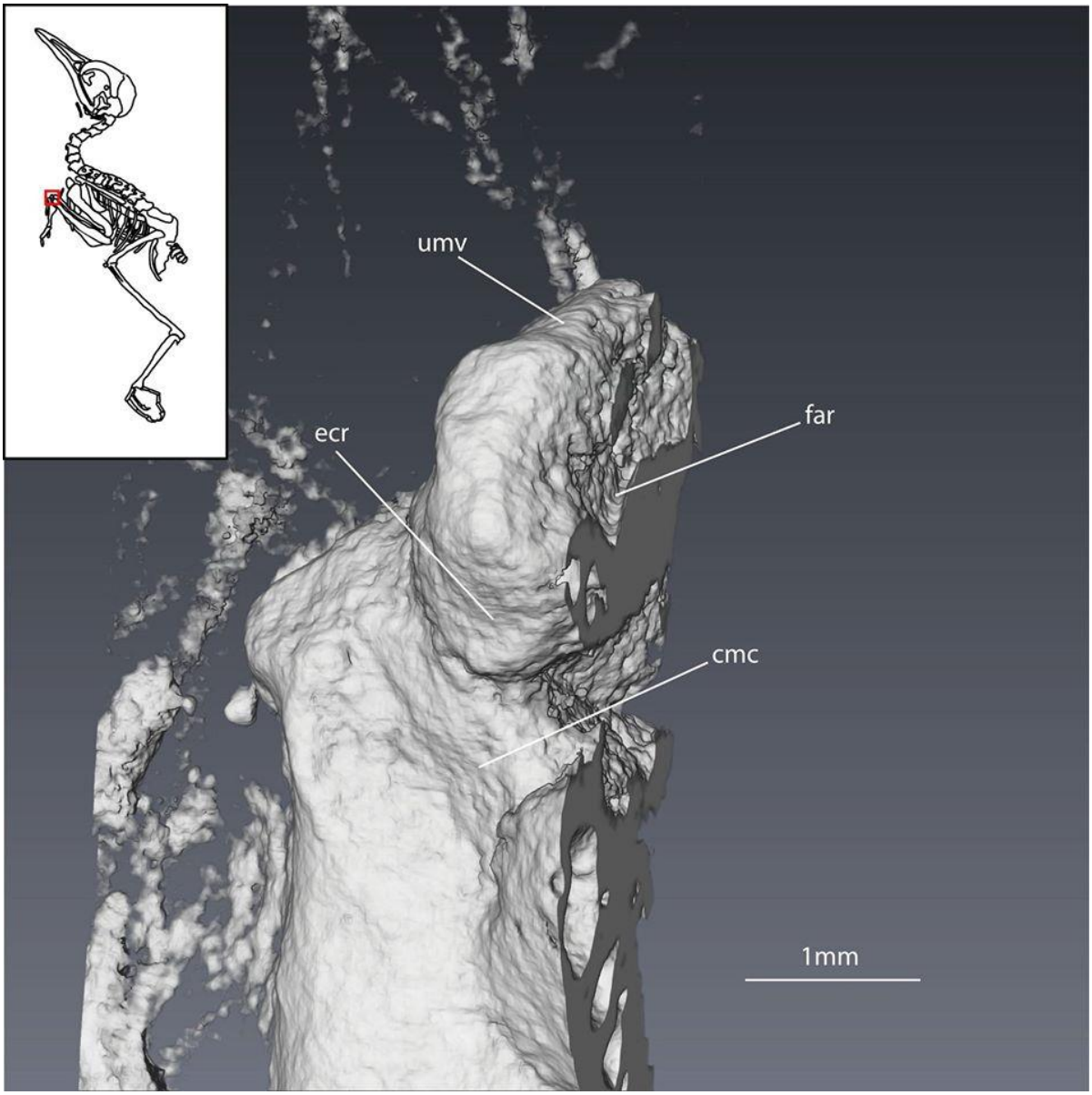

Figure 18: ***Micro CT scan image of the left os carpi radiale in dorsal view, ulna and radius are digitally removed. Abbreviations: cmc: carpometacarpus.;ecr: sulcus for tendon of musculus extensor carpi radialis; far: facies articularis radialis; umv: notch for tendon of musculus ulnometacarpalis ventralis.***

The carpometacarpus is partly preserved, the distal end is missing, but most of the proximal end is preserved in detail. On the proximal end, the processus extensorius is present and shows a hook-like extension. The processus pisiformis is not visible, because it is obscured by the ulna. There is a well-developed processus intermetacarpalis, and this feature is observed in all other described specimens of the Zygodactylidae, and is considered

a synapomorphy of Zygodactylidae and Passeriformes (Mayr, 2008). In contrast to all Passeriformes and most Piciformes, the intermetacarpal process is not fused with the third metacarpal, though they are in articulation (Mayr, 2008). The sulcus tendineus is deep and lies on the dorsal side, and the extension of the sulcus extensorius on the cranial margin is similar to that of SMF-ME 2522 (Mayr, 1998) (see Figure 15). The phalanx digiti alulae and partly the phalanx digiti majoris (the distal end is only preserved as an impression) are present. The phalanx digiti minoris is heavily crushed and no details can be observed. The phalanx digiti majoris is long and slender like many other zygodactylids. The carpometacarpus of the Zygodactylidae commonly exhibits a small processus dentiformis (Mayr, 1998, 2008), but this process is either missing or not preserved in the specimen.

3.2.3 Pelvis and Hind limb

The synsacrum is crushed, but it is well enough preserved in the caudal end to see details. The ilium show signs of crushing and is orientated in the lateral view, so it is only partly exposed. The left ischium and left pubis is well preserved in the specimen, and the pubis is similar in length to that of the other previously described *Primozygodactylus* (see Figure 19), and is longer than the ischium. The ischiopubic fenestra in the specimen is similar to the Passeriformes. There are five free caudal vertebrae preserved and they are similar to what was observed in other species within the Zygodactylidae (SMF-ME 2018) (Mayr, 1998). It is common for all Piciformes and most Passeriformes to possess seven free caudal vertebrae. The pygostyle is unfortunately missing and strengthens the probability that PMO 212.659 is missing two free caudal vertebrae. The first of the caudal vertebrae is preserved in the articulation view and the neural arch is visible.

The left femur (visible in lateral view) is crushed in PMO 212.659, however, it is in good condition in plate B (visible in medial view). The left femur in plate B shows the facies articular acetabularis, and lies in articulation with the pelvic. The left tibiotarsus is well preserved both in the proximal and distal end. The crista cnemialis cranialis is present, but is obscured by the femur (see Figure 19). The tibiotarsus is slightly bent in the distal end in plate B, but it is uncertain if this is a character or if it is due to preservation.

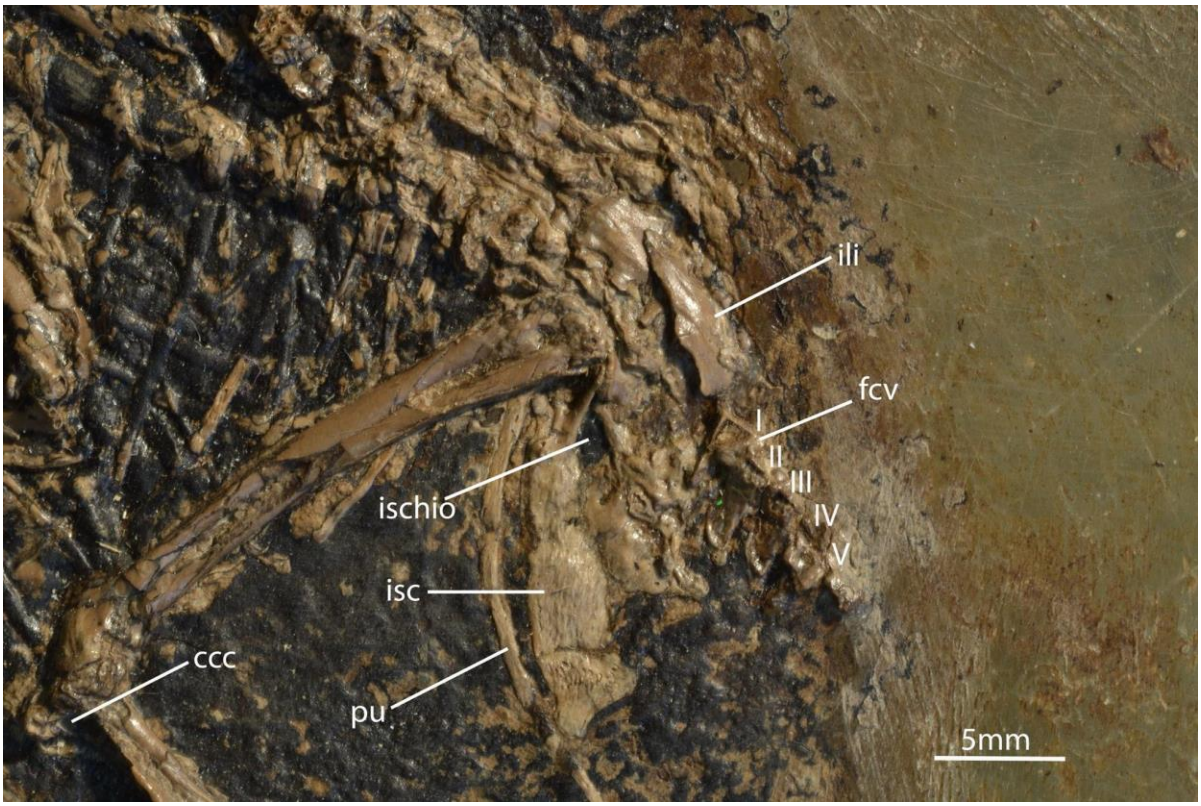

Figure 19: ***Photograph of the pelvic area of*** **Primozygodactylus major*****, PMO 212.659 in lateral view. Abbreviations:*** *ccc****, crista cnemialis cranialis;*** *ischio****, ischiopubic fenestra.*** *I, II, III, IV & V****, are the free caudal vertebrae***

The distal end of the tibiotarsus in PMO 212.659 has a clearly visible depressio epicondylaris lateralis, and is preserved in articulation with the tarsometatarsus. The fibula is about 1/2 of the length of the tibiotarsus in this specimen, and is therefore shorter than that of the holotype, SMF-ME 1758a (Mayr, 1998). Tibiotarsus is the longest hind limb bone, which is similar to the other previously described *Primozygodactylus* (Mayr, 1998; Mayr & Zelenkov, 2009). The central part of the tarsometatarsus is quite crushed and flattened in specimen PMO 212.659, but it is preserved in the proximal and distal end. The proximal end of the tarsometatarsus has a hook-like process on the caudal side, and it is possible that this is the crista medialis hypotarsi (see Figure 20). It was attempted to retrieve more information with the use of the micro CT scanner, but unfortunately the results did not give any further details. Figure 20 shows view of the proximal end of the tarsometatarsus to reveal the details of the hypotarsus. Figure 21 shows previous analysis of the morphology of the hypotarsus in zygodactylids. It is uncertain if the canal for the tendon of m. flexor digitorum longus is present in PMO 212.659 (see Figure 20)

The presences of a large trochlea accessoria, suggest a zygodactyl foot and with the fourth toe in a retroverted position it is safe to assume that PMO 212.659 was zygodactyl. This is a diagnostic character for all zygodactylids (Mayr, 1998, 2008). All four pedal phalanges of the left foot can be observed, and are in articulation. The first phalanx is

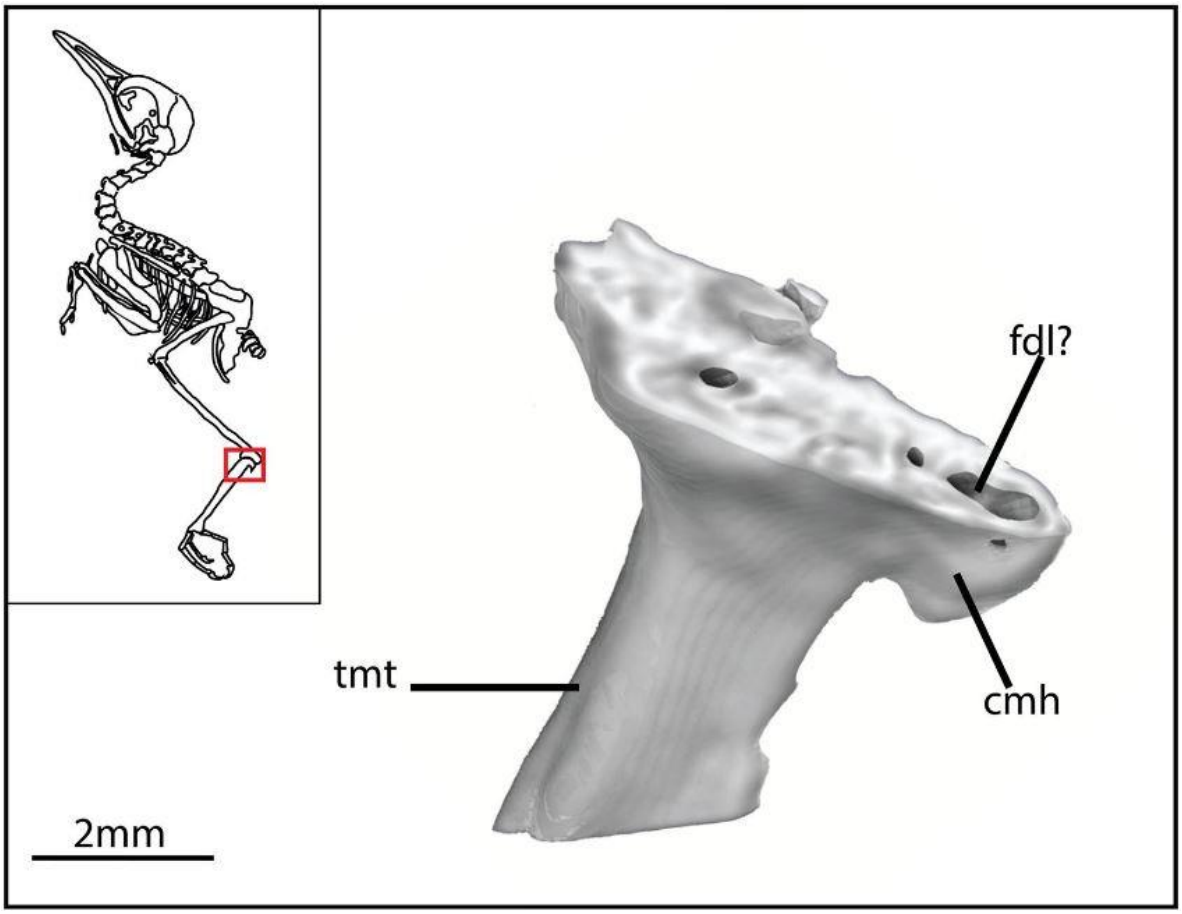

Figure 20: ***Micro CT scan of the tarsometatarsus on the level of the hypotarsus, the cross-section is in oriented in proximal view. Abbreviation:*** *cmh,* ***crista medialis hypotarsi;*** *fdl,* ***canal for tendon of musculus flexor digitorum longus;*** *tmt,* ***tarsometatarsus.***

underlying the second, but is well visible in the CT scan. The phalangeal formula is normal, with digit I being the shortest, digit III the longest and digit IV being only slightly shorter than the third (see Figure 22). The unguals are curved, which is common in arboreal birds (Feduccia, 1999). A sulcus on the dorsal surface of the craniolateral convexity of the tarsometatarsus shaft, just above the trochlea metatarsi IV (see Figure 22A and C) is seen in PMO 212.659. It is most likely to be the distal vascular foramen.

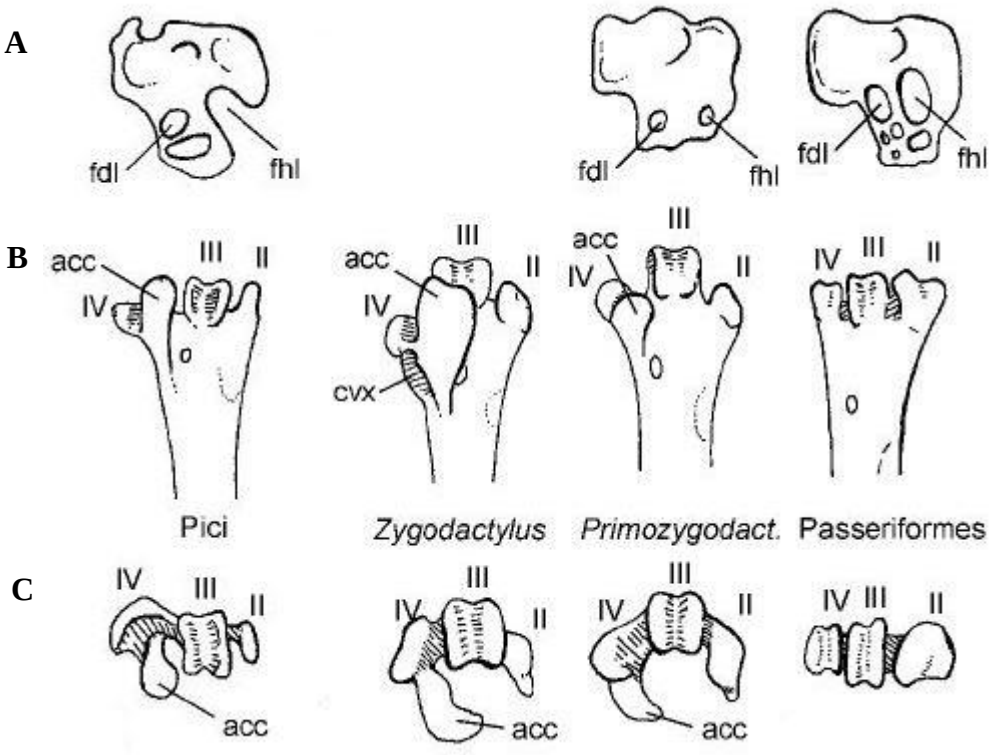

Figure 21: ***Sketch of the tarsometatarsus in proximal (A), plantar (B) and distal (C). All figures are taken from Mayr, (2008). Abbreviations:*** *acc,* ***trochlea accesoria;*** *cvx,* ***convexity on margo lateralis;*** *fdl,* ***canal for tendon of musculus flexor digitorum longus;*** *fhl,* ***canal for tendon of musculus flexor hallucis longus***

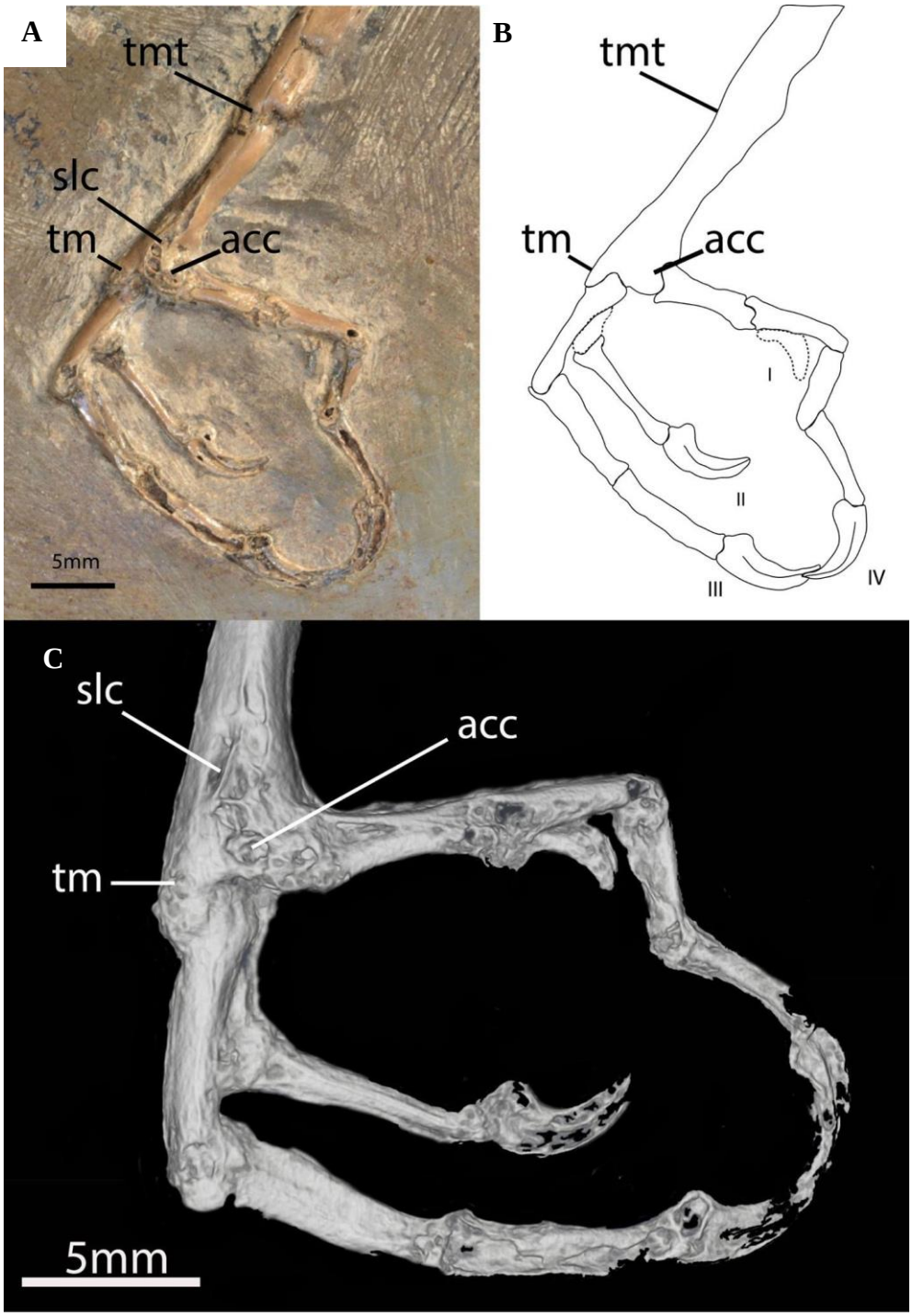

*Figure 22 A-C**: A is a photograph of the left tarsometatarsus of PMO 212.659, orientated in lateral view.** B, line drawing of the distal end of the left tarsometatarsus and the phalanges. C is a CT scan of the distal end of the left tarsometatarsus of PMO 212.659 in lateral view. Abbreviations:* acc*, trochlea accessoria;* tm*, trochlea of metatarsi III;* slc*, sulcus on the dorsal surface of craniolateral convexity;* tmt*, tarsometatarsus.*

3.2.4 Other notable features

Like in a few other *Primozygodactylus* fossils seeds are preserved as former stomach content (Mayr, 1998). These seeds are located slightly to the left of the ulna (between the ulna and carpometacarpus) (see Figure 23). In Plate B, the specimen has preserved feathers countering the head.

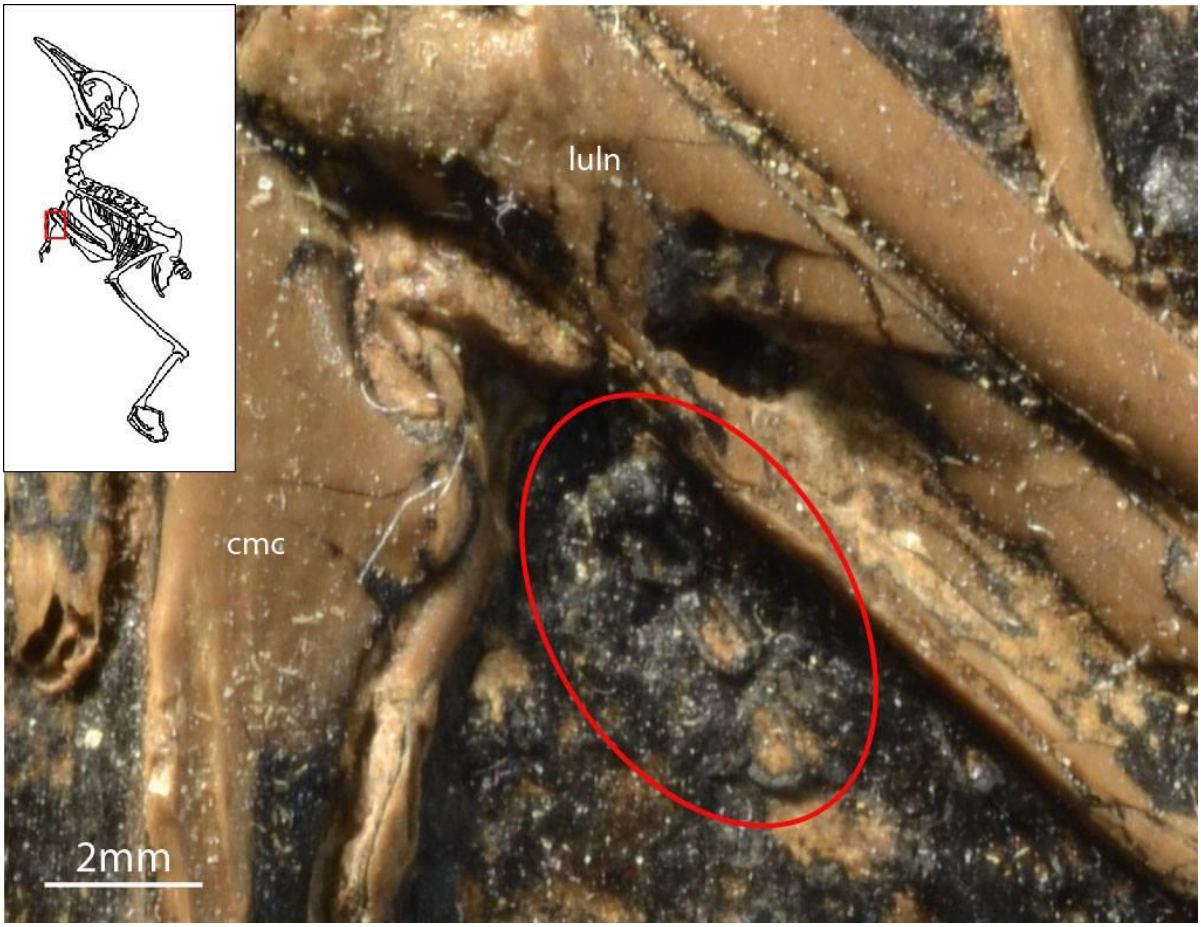

Figure 23: ***Photograph of PMO 212.659. The red circle indicates the seeds preserved in the specimen. Abbreviations:*** *cmc****, carpometacarpus;*** *luln,* ***left ulna.***

4. Discussion

PMO 212.659 exhibits many of the characteristics of *Primozygodactylus*, such as a wide triangular nasal opening, large processus intermetacarpalis of the carpometacarpus, large crista bicipitalis, large trochlea accessoria, elongated tarsometatarsus, and stout pedal phalanges (as compared with *Zygodactylus*). It is the third specimen of *Primozygodactylus major* found. PMO 212.659 is almost identical to the holotype specimen SMF-ME 1758. Although the skull of SMF-ME 1758 is a bit more deformed, it allows the recognition of more osteological information than that of PMO 212.659. The hind limb measurements are almost identical (see Table 3), and the same is true for those of the shoulder girdle and the wing proportions (see Table 2). PMO 212.659 differs from all species of *Zygodactylus* by having a slightly shorter tarsometatarsus – although the bone still exceeds the humerus length – and in that the trochlea accessoria is less bulbous. PMO 212.659 has curved ungual phalanges, which suggests a more arboreal way of living compared to the *Zygodactylus*, which has straighter ungual phalanges and longer pedal digits (Mayr, 2008).

4.1 New data on skeletal elements of *Primozygodactylus*

4.1.1 Quadrate

The quadrate is the best preserved bone in specimen PMO 212.659, and although preservation of quadrates in bird fossils is common, the bone is usually ignored (Elzanowski & Stidham, 2010). However, preservation of the quadrate in zygodactylids has been rather scarce, with only a few of the quadrates being preserved so far and only in the lateral view. The micro CT scans proved to be of great help when describing the quadrate of PMO 212.659. There are many features that would not have been possible to see in the articulated fossil, like the shape of the otic head of the bone.

This study presents for the first time an almost complete reconstruction of the quadrate of *P. major*. The quadrate reveals interesting new features not seen earlier in the Zygodactylidae, but because of the uncertainties in the digital reconstructions, some of these have to be verified in future studies. One of the most interesting feature found in PMO 212.659 is a distinct feature seen in the Upupiformes, the flange of the laterocaudal condyle

(Elzanowski & Boles, 2015). The Upupiformes are the only “higher land birds” that exhibits this feature. However, PMO 212.659 and lacks some of the important features found in the Upupiformes, which have a basal position within the Picocoraciae (Ericson et al., 2006; Hackett et al., 2008). The orbital process in PMO 212.659 is directed rostrodorsally, like the majority of birds (Elzanowski & Boles, 2015). This is different from the Upupiformes, where the orbital process is directed rostroventrally.
The most notable feature in the Passeriformes, the sister taxon of the zygodactylids, is a long and elongated orbital process. Zygodactylids, however, seems to lack this long and elongated orbital process. In specimen PMO 212.659, the orbital process is short and stout, but this may be an artefact of preservation. The 3D model revealed that the process was heavily crushed (see Figure 11B). However, it is peculiar that the short process is seen in another zygodactylid, *Eozygodactylus americanus* (USNM 299821). It is worth noting that the process in USNM 299821 is only partially visible in the lateral view, and further studies are required to clarify the state of the orbital process in zygodactylids.

Mayr (1998) mentions that the capitulum oticum is wide in SMF ME 1758a and a similar feature is seen in PMO 212.659. The capitulum oticum protrudes further medially than that of the Passeriformes, and shows similarities to Upupiformes, Psittaciformes, Charadriiformes, Falconiformes. Upupiformes have a wide capitulum oticum with an extreme medial protrusion, and common has a depression between the capitulum squamosum and oticum, the vallecula intercondylaris. It is uncertain if *Primozygodactylus* has this feature, but there are indications that *Primozygodactylus* does not have this feature. In caudal and rostral view of the quadrate of PMO 212.659 (see Figure 11C and D) there is a slight incline between the two capitula, with a hinge connecting them, and a depression is not seen

A possible new trait for *Primozygodactylus major* is the shape of the facies articularis quadratojugalis (the articulation facies for the jugal bone) (see Figure 10). The cotyla quadratojugalis has an even surface with a shallow depression, which is similar to the Coraciiformes, Piciformes and Psittaciformes (Samejima & Otsuka, 1987). Another new trait for *Primozygodactylus major* is the arrangement of the condylus mandbularis laterocaudalis and the condylus mandibularis medialis seen in ventral view (see Figure 11F), and is similar to the Passeriformes and Piciformes. PMO 212.659 has a large laterocaudale condyle, with a

small depression between the lateralocaudal and medial condyle. The medial condyle is long and extends both ventrally and rostrally. However, although this resembles that of the Passeriformes and Piciformes, it is worth to mention that this is a common trait in many modern birds (Samejima & Otsuka, 1987).

The shape of the quadrate of PMO 212.659 in lateral view resembles that of *Eozygodactylus americanus* (USNM 299821) and in the caudal view that of the holotype specimen of *Primozygodactylus major* (SMF ME 1758).

4.1.2 Os Carpi Radiale

The os carpi radiale is a bone that is often ignored when describing fossil birds, but Mayr (2014) recently described this bone in detail in both extant and in some extinct birds. However, whereas the os carpi radiale of *Zygodactylus* has been described in that latter study, the morphology of this bone remain poorly known for *Primozygodactylus*.

The os carpi radiale of PMO 212.659 is similar in size to that of *Zygodactylus luberonensis*, SMF Av 519. Unfortunately, however, it is crushed, which makes some of the details hard to observe in the exposed ventral view (see Figure 17D). Mayr (2014) mentions that the os carpi radiale of *Z. luberonensis* does not exhibit derived features of the Passeriformes, but that the morphology of this bone in zygodactylids likewise supports a position outside the Picocoraciae, and this is true also for *Primozygodactylus.*

The os carpi radiale of Passeriformes has a more complex shape than that of zygodactylids, being narrower ventrally and dorsally, while the os carpi radiale of zygodactylids (PMO 212.659 and SMF Av 519) is wider. A derived feature of Passeriformes, which is absent in zygodactylids, concerns the morphology of the dorsal part of the facies articularis radialis. This forms a marked dorsally projected process, which contributes to a notch for the distal end of the radius (Mayr, 2014). A characteristics of the Picocoraciae that zygodactylids lack is a narrow sulcus for the tendon of musculus extensor longus and, the sulcus for the tendon of musculus ulnometacarpalis ventralis is wide and shallow (Mayr, 2014). CT investigation of the new specimen confirmed that the shape of the

os carpi radiale of *Primozygodactylus* resembles that of *Zygodactylus*. This bone exhibits a similar shape in all zygodactylids, which supports a phylogenetic placement of these birds outside Picocoraciae, as assumed by Mayr (2014).

4.2 Other notable features observed in PMO 212.659

4.2.1 Mandibula

The dentary depression, seen in Figure 9 in the description, is located where a fenestra mandibulae would be present. Weidig (2010) mentions a similar structure in the dentary of specimen USNM 299821, and it looks similar to the observed feature in PMO 212.659. A mandibular fenestra is common in many birds, but there are many birds that do not have one (Baumel & Witmer, 1993). There are currently no zygodactylids that have shown this feature, and this might be a trait, but it is important to consider the few detailed analyses of the cranial skeletons of zygodactylids, so future studies are crucial to determine cranial features.

4.2.2 Tarsometatarsus

The large trochlea accessoria (see Figure 22) is perhaps the most important feature of the Zygodactylidae. The large trochlea in PMO 212.659 is in articulation with the retroverted fourth toe, so there are few characters that can be discerned. The overall shape of the tarsometatarsus is assumed to be similar to *Primozygodactylus* in Figure 21. The sulcus on the distal end of the tarsometatarsus is relatively large and is the foramen vasculare distale. This feature is seen in other *Primozygodactylus* as well, it is best preserved in specimen SMF ME 1074. There are unfortunately few characters that can be distinguished in the tarsometatarsus of PMO 212.659 due to the crushing of the bone.

4.2.3 Hypotarsus

Knowledge of hypotarsus morphology of the Zygodactylidae would be of critical interest for a phylogenetic placement of these birds. Previous studies (Mayr, 2004, 2008) have shown that the zygodactylids have two closed canals for the tendons of m. flexor hallucis longus

and m. flexor digitorum longus, and these features are in strong relation with the Passeriformes (see Figure 21). This hypotarsus morphology differs from that of the Piciformes, which possess only one closed canal for the tendon of m. flexor digitorum longus and an open canal for the tendon of m. flexor hallucis longus (Mayr, 2004, 2008).

Unfortunately, the CT analyses of the hypotarsus in PMO 212.659 did not yield any further data on the hypotarsus morphology of zygodactylids, because the hypotarsus was not as complete as it appeared to be in the fossil. It was scanned twice in hope for better results, but the second scan did not provide any further insights into the morphology of the structure (see Figure 20). The patterns of the canals of the hypotarsus is not visible in PMO 212.659, but the overall shape of the proximal end of the tarsometatarsus is similar to the previously described of *Primozygodactylus* (see Figure 20) (Mayr, 2008).

4.3 Further work with Micro CT scan

The use of micro CT scan in this study has proven to be useful. CT scan makes it possible to see characters and features that otherwise would be hidden and ignored. This study has proven that the use CT scanning gives a huge advantage, when studying bird fossils like those from Messel, where bones cannot be removed from the matrix for detailed study without destroying the bone. Only a single bird is analyzed here, but there are hundreds of bird fossils from Messel in other collections.

There are still many anatomical elements in the zygodactylids that are unknown and with CT scanning more data could be obtained. The sternum in Plate B would be of interest for a further study with micro CT-scan, since the sternum appears to be almost complete and there are details of the sternum of zygodactylids that are unknown. The internal structure of the cranium would also be of interest in many of the fossil birds found in Messel and other fossils from other sites in the world. Similar CT studies have already been done with crocodiles, dinosaurs and birds (Witmer *et al.,* 2008). The main challenge in obtaining morphological data of both the sternum and cranium in Zygodactylidae is the fact that they are small birds and therefore more crushed than larger birds.

5. Conclusion

PMO 212.659 is the third known specimen of *Primozygodactylus major* and is the first zygodactylid to be scanned with a micro CT scanner, and the first Messel bird to be scanned. The micro CT scan provided crucial data for this study and revealed new features in the cranium (quadrate) and the wing region (os carpi radiale) that have not been seen earlier. The quadrate and os carpi radiale was 3D modelled from the data obtained from the micro CT scans. The 3D models made it possible to examine the other side of the bone that would otherwise be hidden by the matrix.

The overall shape of the quadrate however, is similar to the Passeriformes, especially in the caudal view and a rostrodorsally directed orbital process, even though this is a common trait in the majority of birds. The orbital is shorter than that of the Passeriformes, but the CT scan revealed that this process is crushed. However it is peculiar that the short orbital process is also seen in USNM 299821 and this might reveal that zygodactylids had a shorter orbital process than the Passeriformes. A surprising feature seen in the quadrate PMO 212.659 is a unique feature that is only seen in one extant taxa within the "higher land birds". The Upupiformes bears a flange-like margin on the laterocaudal condyle and PMO 212.659 seems to exhibit this feature. Considered that this is a unique feature for the Upupiformes, this might be an artefact created during the construction of the 3D model. A shallow depression is observed on the cotyla quadratojugalis and is a new feature for the *Primozygodactylus.* Another possible feature is the arrangement of the lateral and medial condyles, which articulates with the mandibular. This is however, a trait seen in many birds including the Passeriformes. It was also spotted an extensive lateral trochlea of the medial condyle, which is also common in many non-passerines.

The CT investigation of the os carpi radiale revealed that the bone in *Primozygodactylus* resembles the *Zygodactylus*, thus all zygodactylids probably have a similar shape of this bone. The dentary depression in PMO 212.659 is similar to the groove mentioned by Weidig (2010) in specimen USNM 299821. This feature is located where the mandibular fenestra usually is positioned, but no mandibular fenestra can be observed. There

are currently no observations of a mandibular fenestra in zygodactylids, but still little is known about their cranial skeleton, so it remains uncertain.

The following traits are new for the Zygodactylidae*:*

For the quadrate:

- The capitulum squamosum is situated higher than the capitulum oticum, there is a small slope between them and no vallecular intercondylaris is present.
- The capitulum oticum is wide, which was recognised by Mayr (1998), but PMO 212.659 revealed in this study a more extensively medial protrusion.
- The laterocaudal condyle ends with a sharp-edged flange.
- A shallow depression on the cotyla quadratojugalis.
- The medial condyle exceeds the lateral condyle ventrally
- A large laterocaudale condyle, with a small depression between the lateralocaudal and medial condyle. This is most likely the lateral trochlea of the medial condyle.

6. References

Avizo user's manual and reference manual - Visualization sciences group. (2011). Retrieved from http://www.vsg3d.com website:

Ballmann, P. (1969a). Die Vögel aus der altburdigalen Spaltenfüllung von Winterhof (west) bei Eichstätt in Bayern. *Zitteliana, 1*, 5-60.

Ballmann, P. (1969b). Les oiseaux miocènes de La Grive-Saint-Alban (Isère). *Geobios, 2*, 157-204.

Baumel, J. J., & Witmer, L. M. (1993). Ostelogia. In J. J. Baumel, A. S. King, H. E. Evans & V. Berge (Eds.), *Handbook of Avian Anatomy: Nomina Anatomica Avium* (2nd ed., Vol. 23, pp. 45-132): Publication of the Nuttal Ornithological club.

Bochenski, Z. M., Tomek, T., Bujoczek, M., & Wertz, K. (2011). A new passerine bird from the early Oligocene of Poland. *Journal of Ornithology, 152*(4), 1045-1053. doi: 10.1007/s10336-011-0693-2

Botelho, J. F., Smith-Paredes, D., Nuñez-Leon, D., Soto-Acuña, S., & Vargas, A. O. (2014). The developmental origin of zygodactyl feet and its possible loss in the evolution of Passeriformes. *Proceedings of the Royal Society of London B: Biological Sciences, 281*(1788), 20140765.

Brodkorb, P. (1971). Catalogue of fossil birds: Part 4 (Columbiformes through Piciformes). *Bulletin of Florida State Museum, Biological sciences, 15*, 163-255.

Brühl, L. (1896). Über Verwendung von Röntgenschen X-Strahlen zu paläontologischen diagnostischen Zwecken. *Verhandlungen der Berliner physiologishen Gesellschaft, Achiv für anatomie und Physiologie*, 547-550.

Buness, H., Felder, M., Gabriele, G., & Harms, F. (2005). Explosive Tropical Paradise - geology and geophysics in time lapse. In S. Schaal (Ed.), *Messel Pit Fossil Site: Snapshots from the Eocene. Vernissage* (Vol. 13, pp. 6-11). Vernissage Verlag.

Chiappe, L. M. (2002). Basal bird phylogeny: problems and solutions. In L. M. Chiappe & L. D. Witmer (Eds.), *Mesozoic birds, over the heads of the dinosaurs*: Berkeley: University of California Press.

Chiappe, L. M., & Witmer, L. D. (2002). *Mesozoic birds, over the heads of the dinosaurs*: Berkely: University of California Press.

Cnudde, V., & Boone, M. N. (2013). High-resolution X-ray computed tomography in geosciences: A review of the current technology and applications. *Earth-Science Reviews, 123*, 1-17. doi: 10.1016/j.earscirev.2013.04.003

Cracraft, J. (1988). The major clades of birds. In M. J. Benton (Ed.), *The phylogeny and classification of the tetrapods - Amphibians, Reptiles and Birds* (Vol. 1, pp. 339-361). Oxford: Clarendon Press.

Dyke, G., & Gulas, B. (2002). The Fossil Galliform Bird Paraortygoides from the Lower Eocene of the United Kingdom. *American Museum Novitates, 3360*(3360), 1-14.

El Bay, R., Jacobsy, W., & Wallner, H. (2001). Milankovitch signals in Messel "Oilshales". *Kaupia, 11*, 69-72.

Elzanowski, A. (2013). More evidence for plesiomorphy of the quadrate in the Eocene anseriform avian genus *Presbyornis*. *Acta Palaeontologica Polonica, 59*(4), 821-825.

Elzanowski, A., & Boles, W. (2012). Australia's oldest Anseriform fossil: a quadrate from the Early Eocene Tingamarra Fauna. *Palaeontology*, *55*(4), 903-911.

Elzanowski, A., & Boles, W. (2015). A coraciiform-like bird quadrate from the Early Eocene Tingamarra local fauna of Queensland, Australia. *Emu*, *115*(2), 110-116.

Elzanowski, A., & Stidham, T. A. (2010). Morphology of the Quadrate in the Eocene Anseriform Presbyornis and Extant Galloanserine Birds. *Journal of Morphology, 271*(3), 305-323. doi: 10.1002/jmor.10799

Elzanowski, A., & Stidham, T. A. (2011). A galloanserine quadrate from the Late Cretaceous Lance Formation of Wyoming. *The Auk, 128*(1), 138-145.

Ericson, P., Anderson, C., Britton, T., Elzanowski, A., Johansson, U., Källersjö, M., Ohlson, J. I., Parsons, T. J., Zuccon, D., Mayr, G. (2006). Diversification of Neoaves: integration of molecular sequence data and fossils. *Biology letters, 2*(4), 543-547.

Fain, M. G., Houde, P., & Harrison, R. (2004). Parallel radiations in the primary clades of birds. *Evolution, 58*(11), 2558-2573.

Feduccia, A. (1999). *The origin and evolution of birds* (Vol. 2nd). New Haven: Yale University Press.

Feduccia, A. (2003). 'Big bang'for tertiary birds? *Trends in Ecology & Evolution, 18*(4), 172-176.

Felder, M., Harms, F., & Liebig, V. (2001). Lithologische Beschreibung der Forschungsbohrungen Groß-Zimmern, Prinz von Hessen und Offenthal sowie zweier Lagerstättenbohrungen bei Eppertshausen (Sprendlinger Horst, Eozän, Messel-Formation, Süd-Hessen). *Geol Jb Hessen, 128*, 29-82.

Franzen, J. L. (1985). Exceptional Preservation of Eocene Vertebrates in the Lake Deposit of Grube Messel (West Germany). *Philosophical Transactions of the Royal Society of London. Series B, Biological Sciences, 311*(1148), 181-186. doi: 10.2307/2396982

Franzen, J. L. (2005). The implications of the numerical dating of the Messel fossil deposit (Eocene, Germany) for mammalian biochronology. *Annales de paléontologie, 91*(4), 329-335.

Franzen, J. L., Gingerich, P. D., Habersetzer, J., Hurum, J. H., von Koenigswald, W., & Smith, B. H. (2009). Complete Primate Skeleton from the Middle Eocene of Messel in Germany: Morphology and Paleobiology. *Plos One, 4*(5), 27. doi: 10.1371/journal.pone.0005723

Gabriele, G. (2007). The Messel Maar. In G. Gruber & N. Micklich (Eds.), *Messel: Treasures of the Eocene* (Vol. 1, pp. 23-28). Germany: Hessisches Landemuseum Darmstadt.

Goth, K. (1990). Der Messeler Ölschiefer ein Algenlaminit. *Courier Forshunginstitut Senckenberg, 131*, 1-143.

Habersetzer, J. (1995). Paläontologie. In F. H. Heuck & E. Macherauch (Eds.), *Forschung mit Röntgenstrahlen* (pp. 633-641). Berlin: Springer.

Hackett, S. J., Kimball, R. T., Reddy, S., Bowie, R. C., Braun, E. L., Braun, M. J., Chojnowski, J.L., Cox, W.A., Han, K.L., Harshman, J., Huddleston, C.J., Marks, B.D., Miglia, K.J., Moore, W.S., Sheldon, F.H., Steadman, D.W., Witt, C.C., Yuri, T. (2008). A phylogenomic study of birds reveals their evolutionary history. *Science, 320*(5884), 1763-1768.

Harrison, C., & Walker, C. (1977). Birds of the British lower Eocene. *Tertiary Research Special Paper, 3*, 1-32.

Irion, G. (1977). Der eozäne See von Messel. *Natur und Museum, 107*(7), 213-218.

Jarvis, E. D., Mirarab, S., Aberer, A. J., Li, B., Houde, P., Li, C., Ho, S. Y. W., Faircloth, B. C., Nabholz, B., Howard, J. T., Suh, A., Weber, C. C., Fonseca, R. R., Li, J., Zhang, F., Li, H., Zhou, L., Narula, N., Liu, L., Ganapathy, G., Boussau, B., Bayzid, M. S., Zavidovych, V., Subramanian, S., Gabaldón, T., Gutiérrez, S. C., Huerta-Cepas, J., Rekepalli, B., Munch, K., Schierup, M., *et al.* (2014). Whole-genome analyses resolve early branches in the tree of life of modern birds. *Science, 346*(6215), 1320-1331.

Kalra, M. K., Maher, M. M., Toth, T. L., Schmidt, B., Westerman, B. L., Morgan, H. T., & Saini, S. (2004). Techniques and applications of automatic tube current modulation for CT. *Radiology, 233*(3), 649-657. doi: 10.1148/radiol.2333031150

Kennett, J., & Stott, L. (1991). Abrupt deep sea warming, paleoceanographic changes and benthic extinctions at the end of the Paleocene. *Nature, 353*, 225-229.

Kühne, W. G. (1961). Präparation von flachen Wirbeltierfossilien auf künstlicher Matrix. *Paläontologische Zeitschrift, 35*(3), 251-252.

Legendre, S., & Léveque, F. (1997). Etalonnage de l'échelle biochrono− logique mammalienne du Paléogène d'Europe occidentale: vers une intégration à l'échelle globale. In J. Aguilar, S. Legendre & J. Michaux (Eds.), *Actes du Congrès BiochroM'97* (Vol. 21, pp. 461–473): Memoires et Travaux de l'Institut de Montpellier de l'Ecole Pratique des Hautes Etudes.

Lemoine, V. (1896). De l'application des rayons Röntgen à l'étude des ossements fossiles des environs de Reims. *C R Soc Biol France, 3*(10), 878–881.

Lenz, O. K., Wilde, V., Mertz, D. F., & Riegel, W. (2015). New palynology-based astronomical and revised Ar40/Ar39 ages for the Eocene maar lake of Messel (Germany). *International Journal of Earth Sciences, 104*(3), 873-889. doi: 10.1007/s00531-014-1126-2

Lenz, O. K., Wilde, V., & Riegel, W. (2007). Recolonization of a Middle Eocene volcanic site: quantitative palynology of the initial phase of the maar lake of Messel (Germany). *Review of Palaeobotany and Palynology*, *145*(3–4), 217-242. doi: http://dx.doi.org/10.1016/j.revpalbo.2006.11.001

Lenz, O. K., Wilde, V., & Riegel, W. (2011). Short-term fluctuations in vegetation and phytoplankton during the Middle Eocene greenhouse climate: a 640-kyr record from the Messel oil shale (Germany). *International Journal of Earth Sciences, 100*(8), 1851-1874.

Liem, K. F. (2001). *Functional anatomy of the vertebrates: an evolutionary perspective* (3rd ed.). Fort Worth: Harcourt College Publication.

Livezey, B. C., & Zusi, R. L. (2007). Higher-order phylogeny of modern birds (Theropoda, Aves: Neornithes) based on comparative anatomy. II. Analysis and discussion. *Zoological Journal of the Linnean Society, 149*(1), 1-95.

Manegold, A. (2008). Morphological characters of the tongue skeleton reveal phylogenetic relationships within the Corvidae (Oscines, Passeriformes). *Emu, 108*(4), 321-330. doi: 10.1071/mu08022

Mayr, G. (1998). Coraciiforme und piciforme Kleinvögel aus dem Mittel-Eozän der Grube Messel (Hessen, Deutschland). *Courier Forshunginstitut Senckenberg, 205*, 1-101.

Mayr, G. (2001). The earliest fossil record of a modern-type piciform bird from the late Oligocene of Germany. *Journal für Ornithologie, 142*(1), 2-6.

Mayr, G. (2003). On the phylogenetic relationships of trogons (Aves, Trogonidae). *Journal of Avian Biology, 34*(1), 81-88.

Mayr, G. (2004). The phylogenetic relationships of the early Tertiary Primoscenidae and Sylphornithidae and the sister taxon of crown group piciform birds. *Journal of Ornithology, 145*(3), 188-198. doi: 10.1007/s10336-003-0018-1

Mayr, G. (2005a). Fine Feathered Fossils of the Eocene. In S. Schaal (Ed.), *Messel pit fossil site: Snapshot of the Eocene* (Vol. 13, pp. 38-43): Vernissage Verlag.

Mayr, G. (2005b). The Paleogene fossil record of birds in Europe. *Biological Reviews, 80*(4), 515-542.

Mayr, G. (2008). Phylogenetic affinities of the enigmatic avian taxon Zygodactylus based on new material from the early Oligocene of France. *Journal of Systematic Palaeontology, 6*(3), 333-344. doi: 10.1017/s1477201907002398

Mayr, G. (2009). *Paleogene fossil birds*. Heidelberg: Springer.

Mayr, G. (2011). Metaves, Mirandornithes, Strisores and other novelties–a critical review of the higher-level phylogeny of neornithine birds. *Journal of Zoological Systematics and Evolutionary Research, 49*(1), 58-76.

Mayr, G. (2014). Comparative morphology of the radial carpal bone of neornithine birds and the phylogenetic significance of character variation. *Zoomorphology, 133*(4), 425-434. doi: 10.1007/s00435-014-0236-5

Mayr, G., & Manegold, A. (2004). The oldest European fossil songbird from the early Oligocene of Germany. *Naturwissenschaften, 91*(4), 173-177.

Mayr, G., & Zelenkov, N. (2009). New specimens of zygodactylid birds from the middle Eocene of Messel, with description of a new species of *Primozygodactylus*. *Acta Palaeontologica Polonica, 54*(1), 15-20. doi: 10.4202/app.2009.B103

Mees, F., Swennen, R., Geet, M. V., & Jacobs, P. (2003). Applications of X-ray computed tomography in the geosciences. *Special publication - Geological Society of London, 215*(1), 1-6.

Mertz, D. F., & Renne, P. R. (2005). A numerical age for the Messel fossil deposit (UNESCO World Heritage Site derived from 40Ar/ 39Ar dating on a basaltic rock fragment. *Courier-forschnungsinstitutt Senckenberg, 255*, 67.

Micklich, N., & Drobek, M. (2007). Mining, Excavations, and Preparation. In G. Gabriele & N. Micklich (Eds.), *Messel: Tresasures of the Eocene* (Vol. 1, pp. 15-21). Germany: Hessisches Landemuseum Darmstadt.

Ni, X., Flynn, J. J., & Wyss, A. R. (2012). Imaging the inner ear in fossil mammals: High-resolution CT scanning and 3-D virtual reconstructions. *Palaeontol Electron, 15*, 18A.

Norell, M. A., & Clarke, J. A. (2001). Fossil that fills a critical gap in avian evolution. *Nature, 409*(6817), 181-184. doi: 10.1038/35051563

Reimann, C. K. (2007). Feathered Arboral Residents. In G. Gruber & N. Micklich (Eds.), *Messel: Treasure of the Eocene* (Vol. 1, pp. 131-137). Germany: Hessisches Landmuseum Darmstadt.

Rogers, S. W. (1999). Allosaurus, crocodiles, and birds: Evolutionary clues from spiral computed tomography of an endocast. *Anatomical Record, 257*(5), 162-173.

Röhl, U., Bralower, T., Norris, R., & Wefer, G. (2000). New chronology for the late Paleocene thermal maximum and its environmental implications. *Geology, 28*(10), 927-930.

Samejima, M., & Otsuka, J. (1987). Observations on the Quadrate of Birds. *Japenese Journal of Ornithology, 35*(4), 129-144.

Schaal, S. (2012). Messel *Evolution & Diversity of Life*. Chichester: John Wiley & Sons, Ltd.

Schaal, S., & Schneider, U. (1995). *Chronik der Grube Messel 1965–1995*. Gladenbach: Kempkes verlag.

Schaal, S., & Ziegler, W. (1992). *Messel: an insight into the history of life and the earth* (M. Shaffer-Fehre, Trans.). United states: New york: Oxford University Press.

Schulz, R., Harms, F., & Felder, M. (2002). Die Forschungsbohrung Messel 2001: Ein Beitrag zur Entschlüsselung der Genese einer Ölschieferlagerstätte. *Zeitschrift für Angewandte Geologie, 4*, 9-17.

Selden, P., & Nudds, J. (2012). Grube Messel. In P. Selden & J. Nudds (Eds.), *Evolution of fossil ecosystems* (Vol. 2, pp. 219-231). USA: Elsevier.

Swierczewski, E. V., & Raikow, R. J. (1981). Hind Limb Morpohology, Phylogeny, and Classification of the Piciformes. *The Auk, 98*(3), 466-480.

Weidig, I. (2010). New Birds from the Lower Eocene Green River Formation, North America. *Records of the Australian Museum, 62*(1), 29-44. doi: 10.3853/j.0067-1975.62.2010.1544

Witmer, L. M., Ridgely, R. C., Dufeau, D. L., & Semones, M. C. (2008). Using CT to peer into the past: 3D visualization of the brain and ear regions of birds, crocodiles, and nonavian dinosaurs. In H. Endo & R. Frey (Eds.), *Anatomical Imaging - Torwards a new morphology* (pp. 67-87). Japan: Springer.